

LAPPEENRANNAN TEKNILLINEN YLIOPISTO

School of Engineering Science

Degree in Computational Engineering

Bachelor's thesis

Timo Paappanen

Measurement of magnetic properties of graphite samples

Ohjaaja: Erkki Lähderanta

Abstract

Lappeenranta University of Technology

School of Engineering Science

Degree Program in Computational Engineering

Timo Paappanen

Measurement of magnetic properties of graphite samples

Pages 20, Images 11

Bachelor's thesis

2019

Multiple samples of graphite were given for measurement for the study. Three of them were perforated, and two of them were pure to give a reference point to the perforated samples. The purpose was to measure and determine the magnetic behaviour of these samples using the SQUID magnetometer for measurements.

Using $M(T)$ graphs drawn from the results using the GNU octave open source scripting language, it was found out that the perforated samples showed negligible ferromagnetic behaviour, while the pure samples behaved in a temperature-dependent paramagnetic way.

In addition, by plotting the inverse magnetization by temperature $1/(M(T)-M_0)$ a fit for Curie-Weiss law was attempted, which resulted in low negative Curie temperatures in the range of 0 to -3 K and Curie constant in the range of 0.0009 to 0.0025 K*emu/g.

Table of contents

Abstract.....	2
List of symbols and abbreviations.....	4
1. Introduction.....	5
1.1 Overview.....	5
1.2 Goals and delimitations.....	5
1.3 Structure of the thesis.....	5
2. Theory.....	6
2.1 Types of magnetism.....	7
2.2 Curie-Weiss law.....	9
3. SX700 SQUID magnetometer.....	11
4. Samples.....	13
5. Used programming interface.....	13
6. Measurements.....	14
7. Analysis of results.....	18
8. Conclusions.....	19
9. Sources.....	19
9.1 Image sources.....	20
10. Attachments.....	20

List of symbols and abbreviations

units

M	Magnetization	
m	Magnetic dipole moment	
m	Mass	[kg]
τ	Magnetic moment	[A*m ² , emu]
B	Magnetic flux density	[T, Oe]
Z -moment	Magnetic moment over Z axis	[emu, A*m ²]
M	Z -moment per unit of mass, mass magnetization	[emu/g, (A*m ²)/kg]
χ	Magnetic susceptibility	
χ_{mass}	mass susceptibility	[emu/g, H*m ² /kg]
T_n	Neel temperature	[K]
T_C	Curie temperature	[K]
C	Curie constant	[]

abbreviations

SQUID	Superconducting Quantum Interference Device
CGS	Centimeter Gram unit system
SI	(abbr. of <i>Système international</i>) International system of units
FC	Field cooling
ZFC	Zero field cooling

1. Introduction

1.1 Overview

Magnetic properties of carbon are a relatively new area of study. Graphite has been found to display some magnetic properties. These properties could have potential uses in different fields. In this study was measured the temperature dependence of magnetization of three different graphite samples, which have been perforated at different temperatures (280, 800 and 1000 K), giving them different physical properties. In addition, two pure graphite samples were measured to make comparisons. The measurements were done using SQUID magnetometer.

1.2 Goals and delimitations

This thesis is mainly based on measurements of several graphite samples obtained from multiple sources. The general aim is to identify the magnetic behaviour of the samples, and compare them to other materials. In addition to this, some external resources are used to get information.

1.3 Structure of the thesis

The Bachelor's thesis consists of eight general sections: This introduction, theory section, introduction to SQUID, description of samples and software, part which describes the measurements, analysis and conclusions. In addition to these, the used sources and attachments are also listed.

Section 2, the theory describes the necessary information to understand the discussed topic. This includes the magnetic units and types of magnetism.

The third part is used to describe the SQUID magnetometer, which was used for making the measurements. This includes the main operation principle and its relevant limitations.

The fourth and fifth part describe the analyzed samples and the software GNU octave used for analysis respectively.

Sixth section describes the general process of how the measurements were done, and how the analyzed graphs were drawn.

In the seventh section analyzes the results gotten in the fifth section.

The eighth and final section introduces the conclusions drawn from this study.

2. Theory

Magnetism is a phenomenon that is part of electromagnetism. There are various units to describe the behaviour of materials in magnetic fields, where the most relevant of them are covered in this section.

There are two mainly used sets of units for magnetic measures: the international system of units (SI-units) and the CGS (Centimeter Gram System) unit system, which is based on the international system of units. In this study, the CGS units are used primarily for the magnetic measures.

Magnetic moment is a vector which relates to the aligning torque an external magnetic field applied to an object. The relationship between these is:

$$\boldsymbol{\tau} = \mathbf{m} \times \mathbf{B} \quad (1)$$

Where $\boldsymbol{\tau}$ is the torque, \mathbf{m} is the magnetic moment and \mathbf{B} the external magnetic field.

From this torque we can derive magnetization \mathbf{M} , which is a measure that expresses the density of magnetic dipole moments in a given material. It is a vector field unit and is calculated as follows:

$$\mathbf{M} = d\mathbf{m}/dV \quad (2)$$

Where \mathbf{m} is the magnetic dipole moment and dV represents a volume element.

The relation between magnetization of a medium and the applied external magnetic field is known as (magnetic) susceptibility, which is defined as relationship magnetization and magnetic field[1]:

$$\chi = M/H \quad (3)$$

Where χ is susceptibility, M is magnetization and H the external magnetic field (unit $[A/m]$ (SI) or Oe (cgs)). Susceptibility is a dimensionless quantity, meaning it doesn't have an associated unit.

Magnetic moment can be divided into three axial components: m_x , m_y and m_z component. Given a sample of mass m with a Z -moment of m_z , the mass-magnetization can be calculated as follows:

$$M = Z\text{-moment}/m \quad (4)$$

Where M is the mass magnetization (unit $A \cdot m^2/kg$ (SI), or emu/g CGS)), Z -moment (unit $Wb \cdot m$ (SI) or emu (CGS)) and m is mass (unit kg (SI) or g (CGS)). It represents the magnetic moment per unit of mass. In addition, mass susceptibility χ_{mass} has the same dimension as mass magnetization.

When studying unknown materials, their magnetic properties can be systematically determined by sweeping them in their safe-temperature range in a low magnetic field (50-100 Oe). This process serves only as a starting point, and more detailed studies are required to obtain the properties from areas of particular interest.

2.1 Types of magnetism

There are four different main types of magnetic behaviour: paramagnetism, diamagnetism, ferromagnetism, and antiferromagnetism. All of these are differentiated by how the material reacts to an external magnetic field.

Paramagnetism is identified by material having a linear inverse-temperature-mass-magnetization curve (figure 1). Paramagnetism is also reversible, meaning that the $M(T)$ plots for heating paramagnetic samples are the same as the curve when the same sample is cooled down. It is the simplest type of magnetic behaviour.

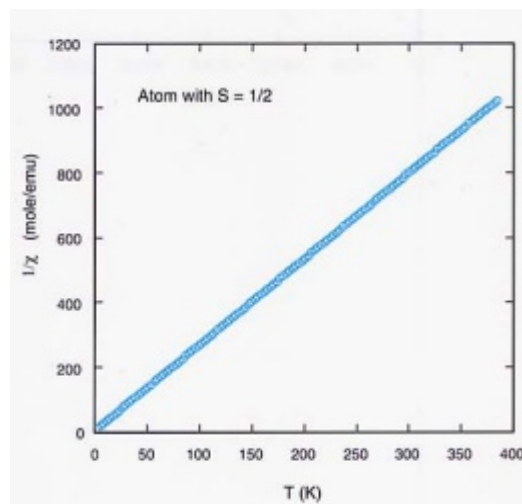


Figure 1: Inverse susceptibility ($1/\chi$) plotted against temperature (T) for a hypothetical, nearly ideal paramagnetic material. Note the linear relationship between $1/\chi$ and T .

Diamagnetism on the other hand is identified by the material having a negative magnetism and a reversible $M(H)$ plot (figure 2). This means that the susceptibility (χ) is negative. There are generally two types for diamagnetism: paired electron contribution to the magnetic behaviour and superconductivity.

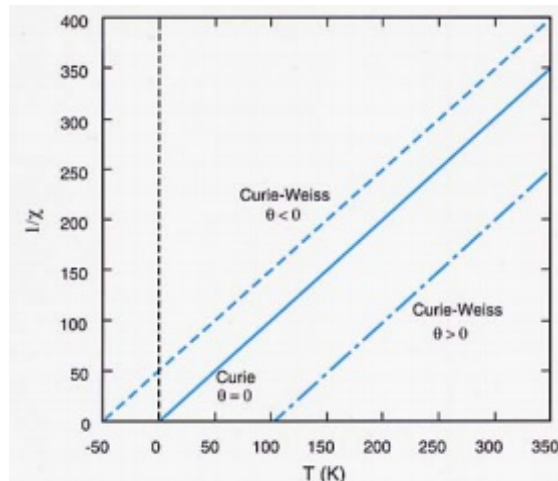


Figure 2: Inverse susceptibility ($1/\chi$) plotted against temperature (T) for a hypothetical diamagnetic materials with marking of Curie-Weiss factors (θ).

Ferromagnetism is an important type of magnetism. It has a distinctive $M(H)$ and $M(T)$ curves which are not linear, and have different heating and cooling curves, ie, the curves are not reversible (figure 3). This lack of reversibility is also called magnetic hysteresis. Ferromagnetic materials also exhibit a Curie temperature T_C , above which they show Curie-Weiss behaviour and behave like paramagnetic materials.

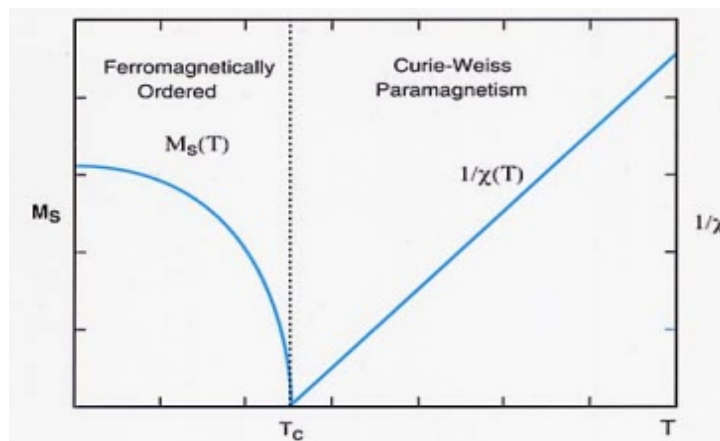


Figure 3: Inverse susceptibility ($1/\chi$) plotted against temperature (T) for a ferromagnetic material. Above Curie temperature (T_c), the material exhibits Curie-Weiss behaviour and is paramagnetic. Below this temperature, χ is both field and history dependent and is not a useful parameter.

Antiferromagnets have the property of having their magnetic moments aligned opposite to each other, which results them canceling each other out. This results in small values of M . Antiferromagnets behave essentially like paramagnets, but also have the irreversibility typical to ferromagnets, and thus have the same parameters (H_c , M_{rem} , M_s) to describe the behaviour. For antiferromagnetic materials there exists a specific temperature called the Néel temperature (T_n),

above which the material becomes paramagnetic (figure 4). [2]

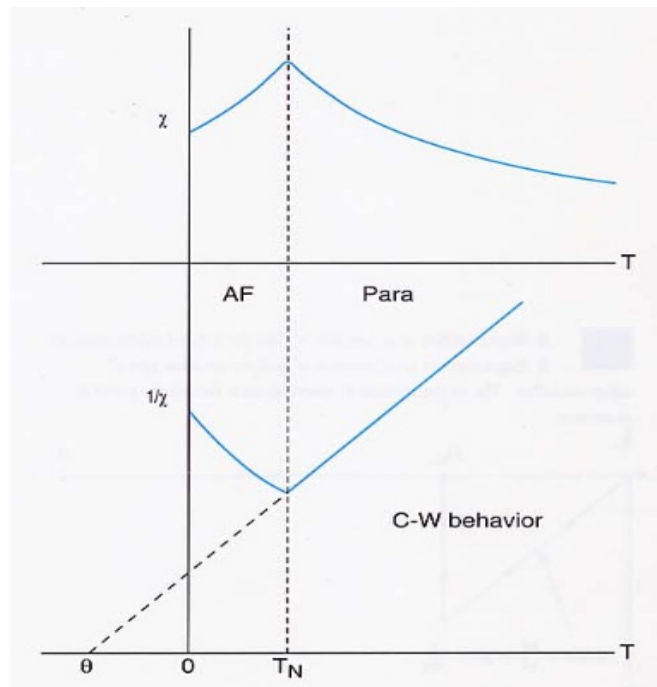


Figure 4: Temperature-susceptibility/inverse susceptibility graphs for an antiferromagnetic material. The neel temperature is marked with T_n

Table 1: Table for classifying magnetic materials based on their properties (source: [2])

Class	χ dependence on B	Temperature dependence of magnetization	Hysteresis	Example	χ
Diamagnetic	No	No	No	water	$-9.0 \cdot 10^{-6}$
Paramagnetic	No	Yes	No	Aluminium	$2.2 \cdot 10^{-5}$
Ferromagnetic	Yes	Yes	Yes	Iron	3000
Antiferromagnetic	Yes	Yes	Yes	Terbium	$9.51 \cdot 10^{-2}$
Ferrimagnetic	Yes	Yes	Yes	MnZn	2500

2.2 Curie-Weiss law

When plotting an inverse susceptibility-temperature curve for diamagnetic materials and ferromagnetic materials above certain temperature, the result is a straight line. For ferromagnetic materials, there is also a discontinuity at a certain temperature called the Curie temperature T_C . This behaviour is described by Curie-Weiss law. For ferromagnetic materials in the paramagnetic region above the curie temperature T_C and paramagnetic materials this can be expressed as:

$$\chi = \chi_0 + C/(T-T_C) \quad (5)$$

Where χ is susceptibility, C is curie constant, T is temperature and T_C is Curie temperature.

This behaviour arises from the fact that the alignment of magnetic moments is dependent on temperature: Below T_C the magnetic moments are aligned and the material behaves in ferromagnetic way, having non-linear relationship between $1/\chi$ and T .

Because mass magnetization is directly propotional to mass susceptibility, Curie-Weiss law can also be expressed in terms of mass magnetization:

$$M = M_0 + C/(T-T_C) \quad (6)$$

3. SX700 SQUID magnetometer

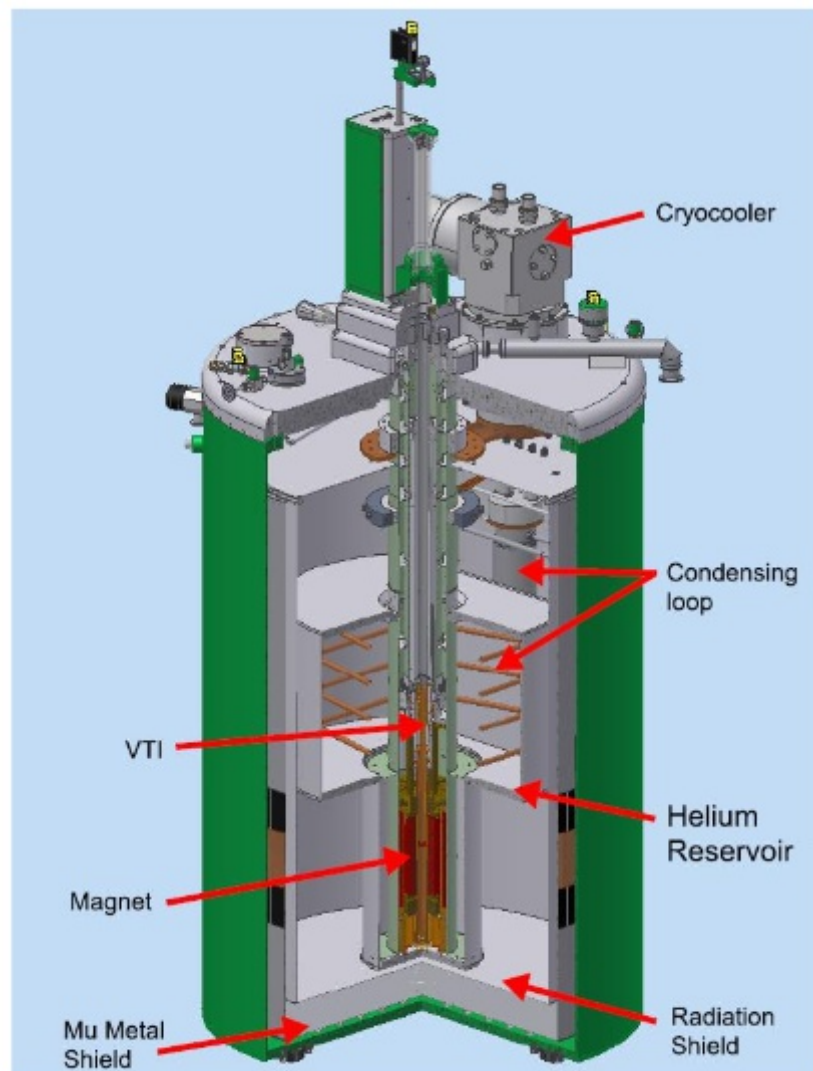


Figure 5: Illustration of SQUID's internal structure.

SX700 SQUID (Superconducting Quantum Interference Device) is an integrated instrument designed for magnetic measurements [3]. The sample temperature can be set from as low as 3 K to up to 400 K, and the magnetic field that can be applied from the superconducting magnet ranges from 0 T to 7 T. The temperature is adjusted by using liquid helium in the helium reservoir.

SQUID is sensitive for magnetic flux, and detects it by converting it to AC/DC electrical signal with Josephson junction. Electrons are known to have wave like properties. Passing through the Josephson junction the wave is split into two, pass through the junction and then converge back together. Without external magnetic field, the branches are equivalent and the phase difference of arriving waves are equal. However, in the presence of external magnetic field, a circulating superconducting current will be induced in the ring. This current will be added to one of the splitted

electron currents, and subtracted from the other, causing a phase difference between the two arriving waves. This causes a voltage oscillation with a period Φ_0 , which can be measured and used to determine the magnetic flux going through the junction (figure 6).

The main variables the magnetometer can control is sample temperature T and magnetic field B , which are controlled by liquid helium and superconductive magnet, respectively. During the measurements, a rod holding the sample is moved up and down by a stepper motor in order to trigger the magnetic response from the magnetic field.

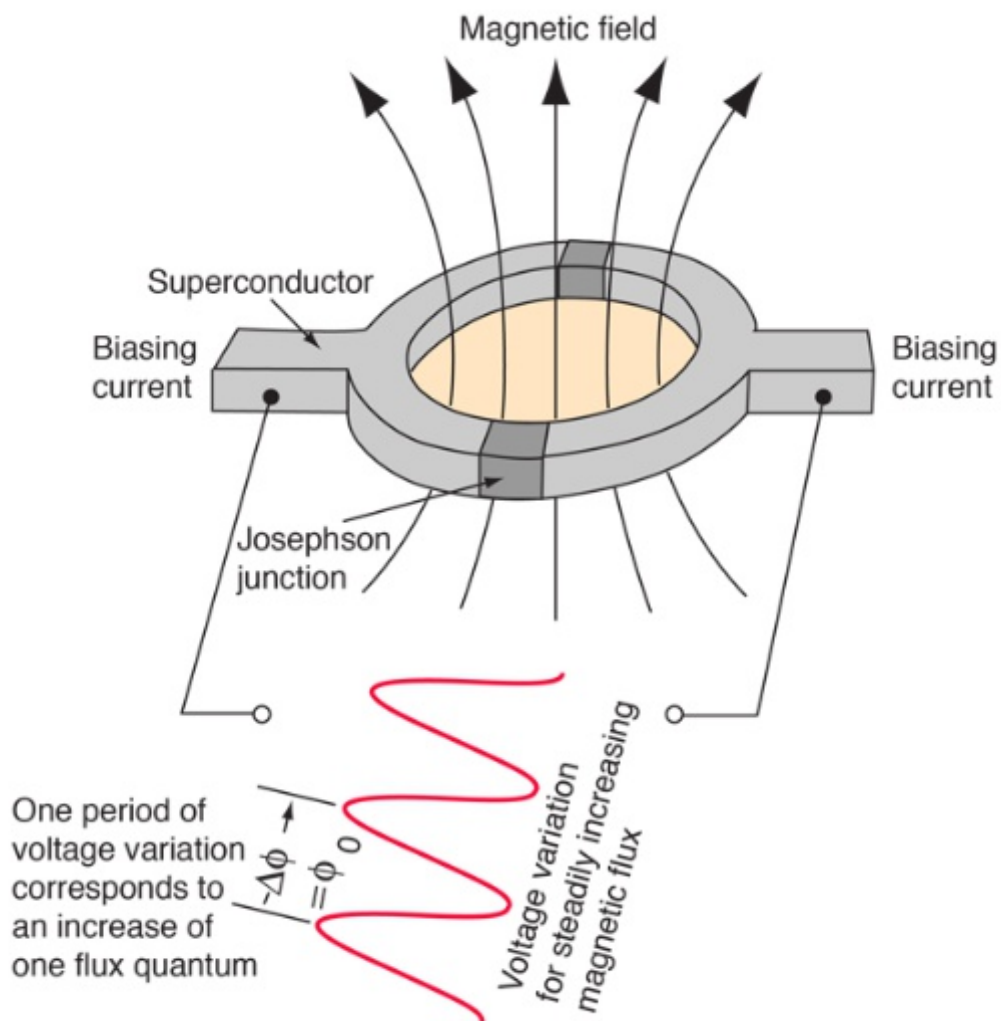


Figure 6: Operation principle of SQUID



Figure 7: Squid magnetometer and electronic rack

4. Samples

There were a total of five graphite samples that were measured, each with distinct properties. The first three samples were handled in a process called perforation, in which the flakes get punctured with small holes. This process was carried at temperatures of 280, 800 and 1000 °C respectively for samples 1, 2 and 3. The total masses of these samples were weighed to be 0.0136 g (sample #1), 0.0112 g (sample #2) and 0.0112 g (sample #3) when put inside the mounting capsules.

The fourth and fifth samples were pure graphite samples from Novosibirsk, Russia and a commercial sample from Italy with masses of 0.05180 g and 0.086 g respectively.

5. Used programming interface

The open source scripting language and software GNU octave (first released in 1993) was selected

for plotting the results. The software is designed for scientific use much like its commercial counterpart, matlab, having built in functions for reading data from files, plotting results, handling matrices, mathematical operations, solving linear and nonlinear equations etc[4]. In this work, the data reading and plotting capabilities were primarily used for plotting the results of the measurements.

6. Measurements

The samples which had annealing temperatures of 280, 800 and 1000 °C were put in a capsule by using cleaned equipment taking care not to contaminate them, and then mounted in SQUID after measuring the mass of the samples. After centering the DC-graphs, the temperature sequence was started, which uses a constant magnetic field and a differing temperature to measure magnetization of the mounted sample. Because of the relatively weak magnetic properties of the graphite samples, a strong magnetic field (0.08 T) had to be used to get strong enough signal to measure it reliably. The temperature profile used for the measurements consisted of warming up the sample from 5 K to 300K, and then cooling it back down to 5 K. The same sequence (constant magnetic field of 0.08 T) of temperatures was used for every sample. The results were files, where rows represented the different measurements, and contained data such as the times of measurements, average Z -moments, temperature measurements before and after the measurements, and the magnetic field.

After all of the measurements were done, the mass-magnetization M using the formula (4) for each sample was calculated and plotted with temperature T using GNU Octave on a $M(T)$ plot.

After the first measurements, a second set of measurements were made with smaller temperature step to give more accurate results. The plot for the second mass-magnetization-temperature is as follows (figure 8):

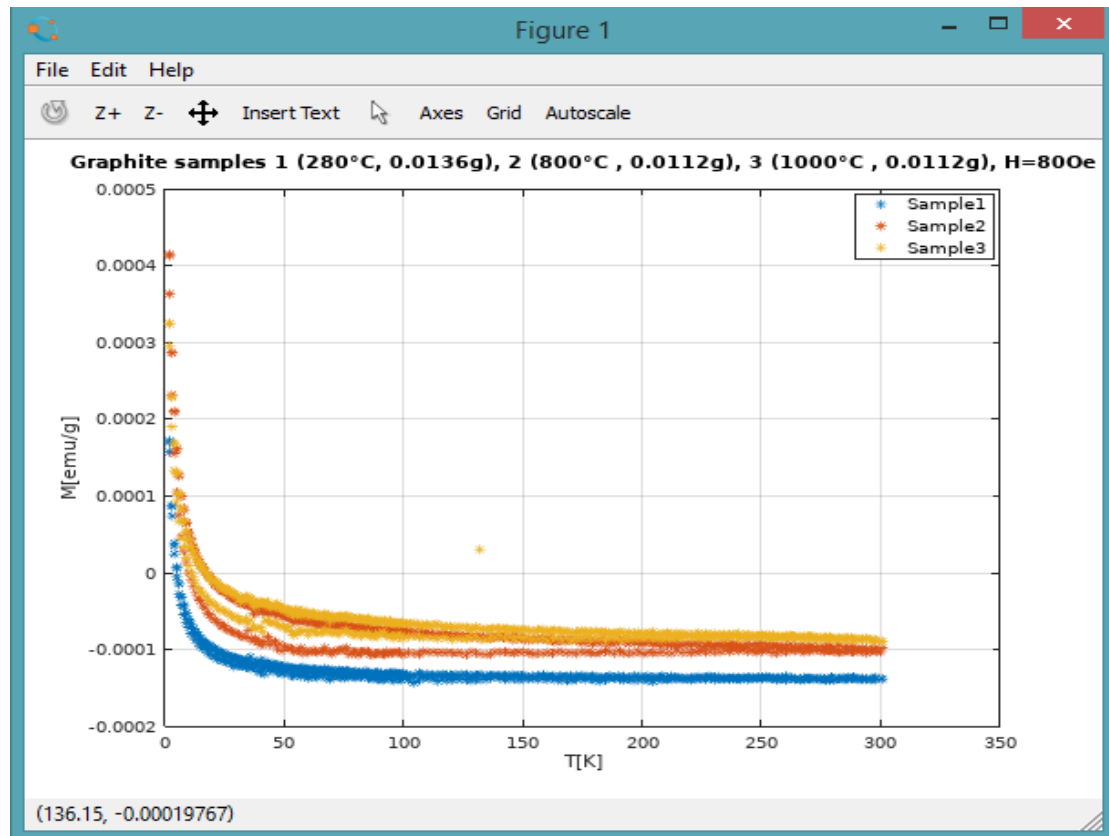


Figure 8: $M(T)$ plot of the second measurements of the perforated graphite samples

After these, two pure graphite samples (commercial RW-A SGL CARBON from Italy and another sample from Russian Novosibirsk's University) were measured in a similar way to give comparison to the three perforated samples. The new results were plotted in to the same $M(T)$ graph, which resulted in the following graph (figure 9).

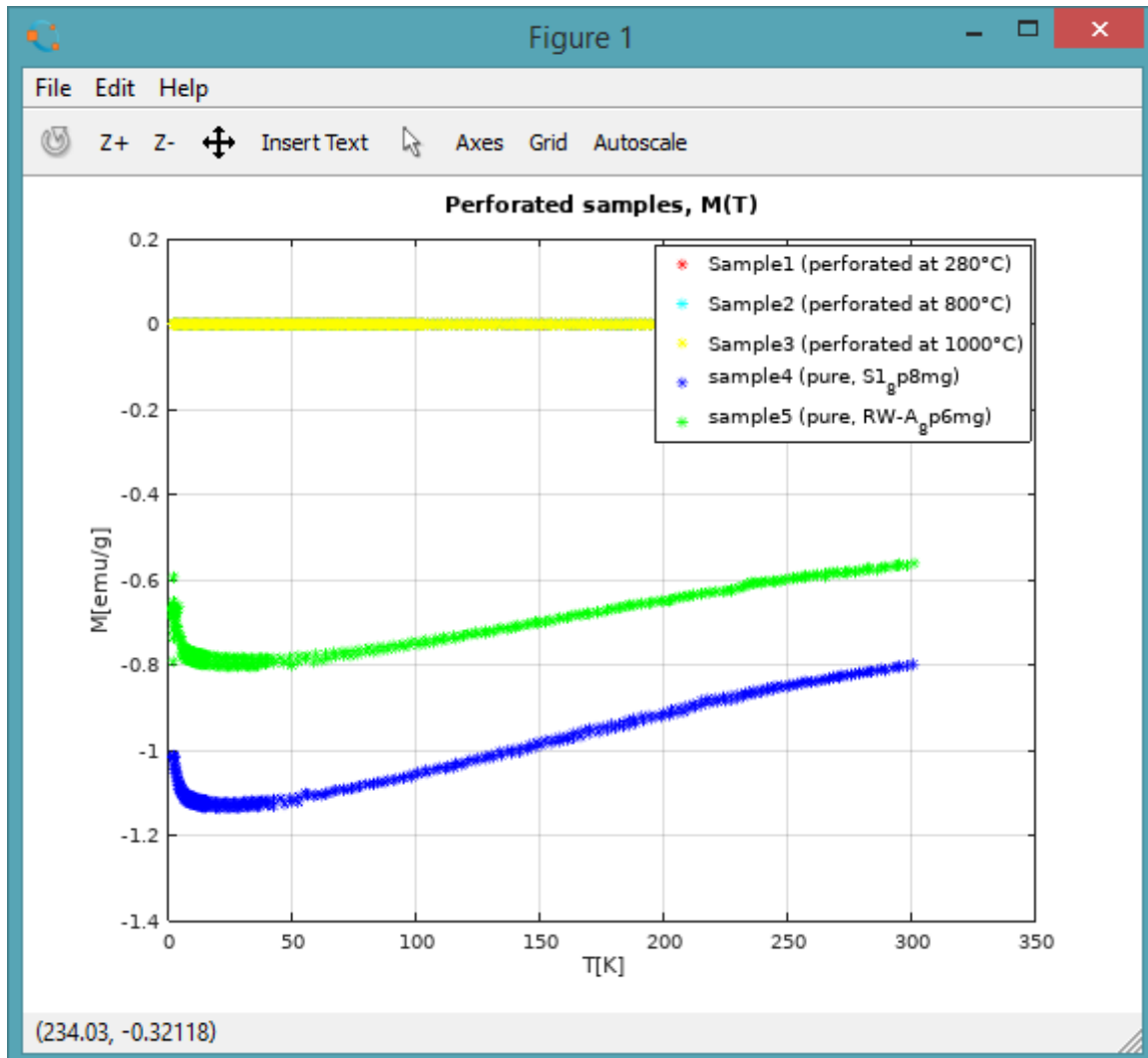


Figure 9: $M(T)$ plot of measurements with pure samples' graphs shown

The first pure sample (sample 4) contained some additional points which were clearly not a part of the measurements, and thus were removed from the plot as outliers.

In addition to regular $M(T)$ plotting, plotting the inverse of mass magnetization allows for analysis of any potential fit for Curie Weiss law (6). For the three perforated samples this results in the following inverse plot (figure 10):

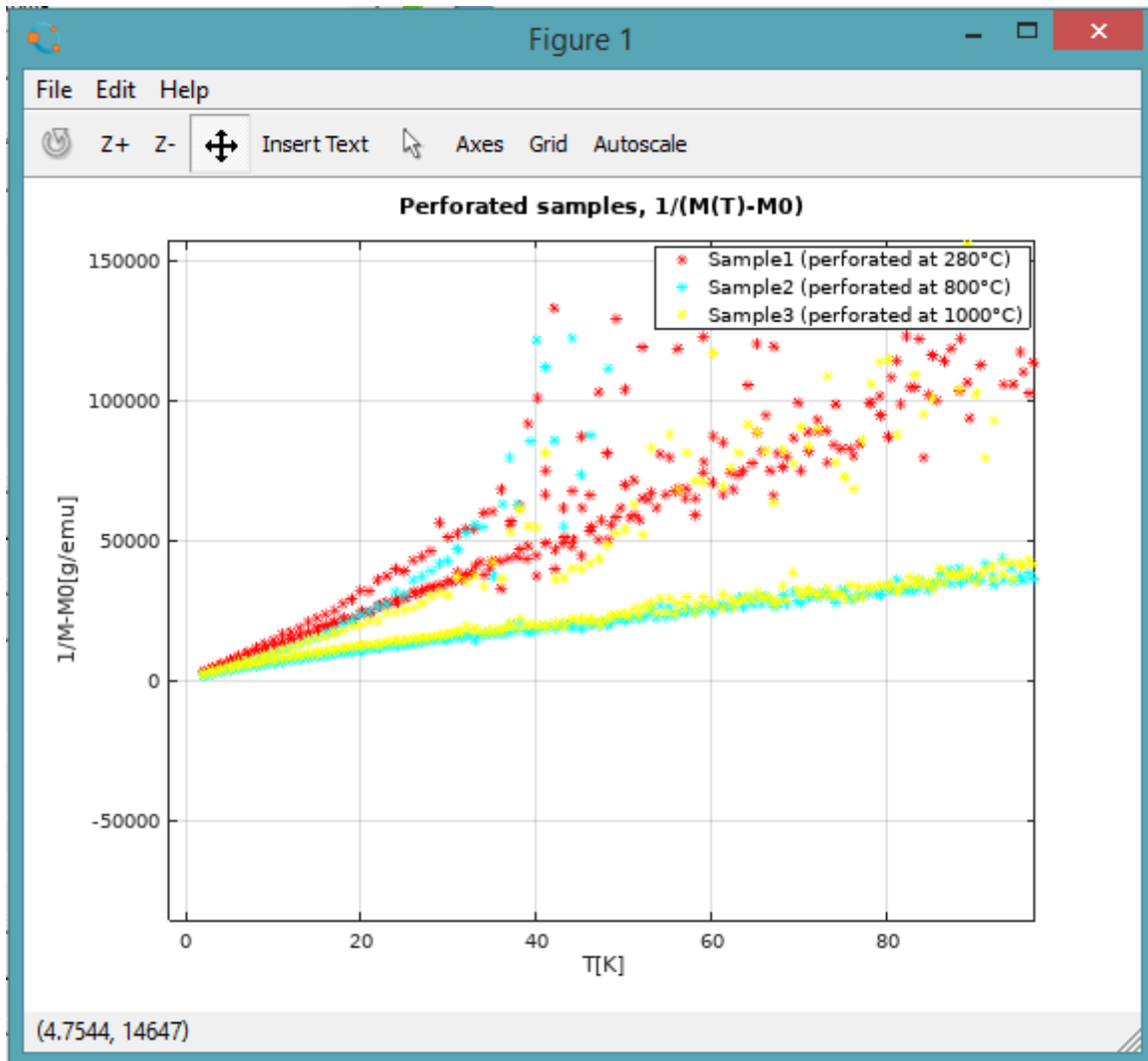


Figure 10: $1/(M(T)-M_0)$ plot of perforated graphite samples, second measurements.

When viewed this way, the inverse magnetization appears as mostly straight lines with points previously near 0 magnetization appearing as noise, and the plot becoming increasingly sparse when moving into higher temperatures. Also the FC and ZFC lines are still distinct from each other. By estimating M_0 from the magnetization curve endpoints ($T=300\text{K}$, saturation point) of figure 8 and adjusting T_C and C , it was possible to make a fit for Curie-Weiss law of these results. M_0 was estimated to be -0.0001398 emu/g , -0.0001017 emu/g and -0.0000895 emu/g for samples 1, 2 and 3.

With this information, manually adjusting variables resulted in the following fits for Curie-Weiss law of the upper linear portions (Samples warming up from 2 K to 300 K) (figure 11):

$$\text{Sample \#1: } 1/(M-(-0.0001398\text{ emu/g})) = (T - 300\text{ K})/ 0.0009\text{ K*emu/g}$$

$$\text{Sample \#2: } 1/(M-(-0.0001017\text{ emu/g})) = (T - 150\text{ K})/ 0.0025\text{ K*emu/g}$$

Sample #3: $1/(M(-0.0000895 \text{ emu/g})) = (T - 500 \text{ K})/ 0.0023 \text{ K*emu/g}$

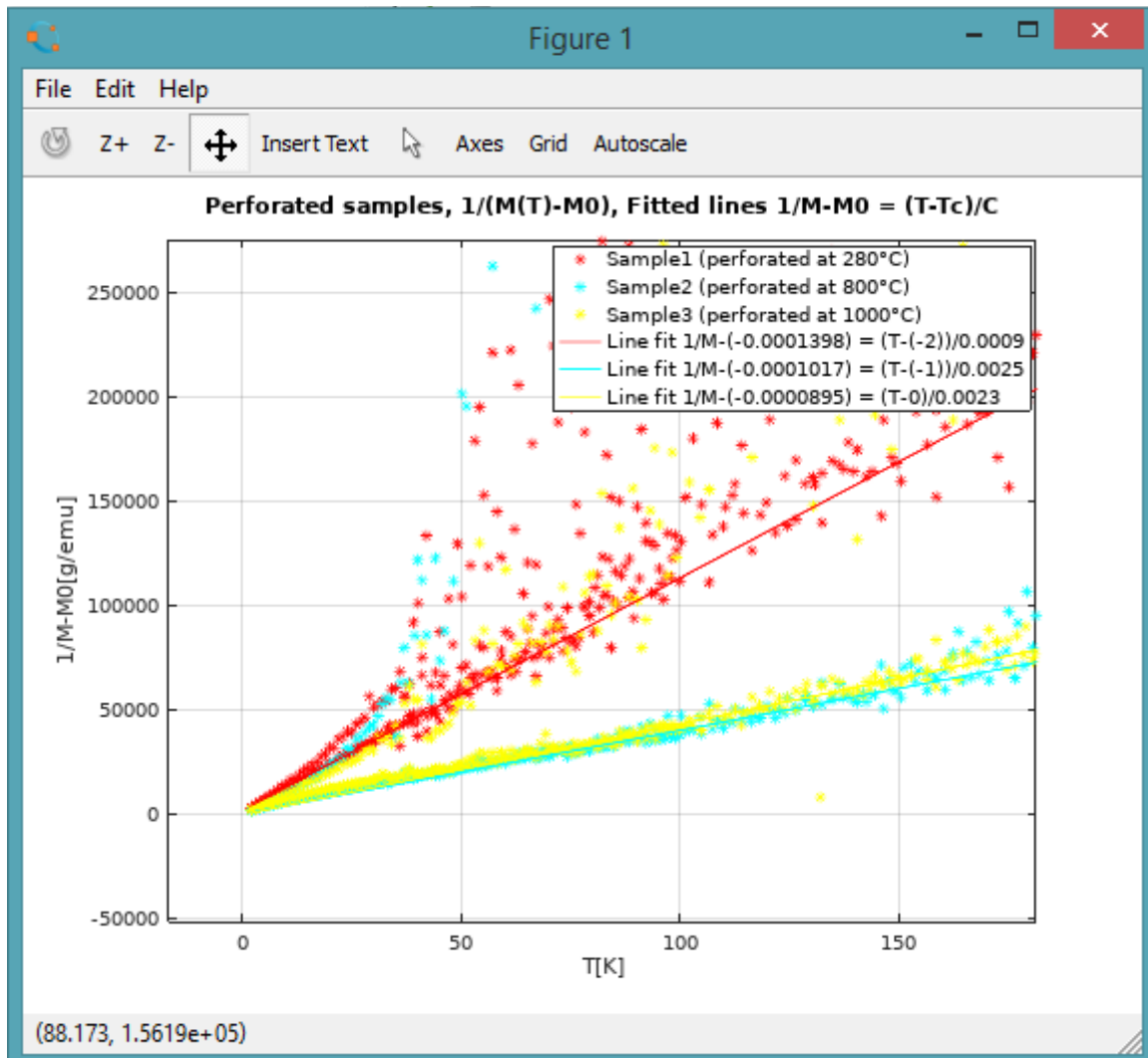


Figure 11: $1/(M(T)-M_0)$ plot with manual fit Curie-Weiss.

7. Analysis of results

Plotting the second measurements in a mass magnetization-temperature graphs produced a magnetization curve, which composes of two parts: field cooling (FC) and zero field cooling (ZFC), which correspond to the cooling and heating parts of the measurement process. These differing curves are indicating the irreversibility characteristic of ferromagnetic materials. It can also be seen that the curves are different for different samples. Second observation is that higher numbered graphite samples had their magnetization points overall higher than lower numbered. Although when comparing to the pure samples magnitude of magnetization, the ferromagnetism is overall

negligible or does not actually exist.

When comparing to some other materials, the mass magnetization of the samples is relatively high. For example, Bismuth, has a mass susceptibility of -1.35×10^{-6} emu/g at temperature a of 20 C [5]. Comparing the measured samples (with of mass magnetization around 1×10^{-4}), this is around 100 times larger magnetization.

On the other hand, pure samples show a lot stronger negative mass magnetization. The magnetic behaviour for these appears to be temperature dependent paramagnetism.

8. Conclusions

We found out the magnitude and type of general order of the magnetic behaviour of the three perforated graphite samples in this study. In addition, we compared the results to similar measurement of pure graphite samples. We found out that the perforated samples showed a very small magnetic response, while the pure samples behaved in temperature dependent paramagnetic way. With further studies, additional and more accurate dimensions of the properties could be determined.

Because graphite is a common and cheap material, the magnetic properties of it could be useful in different applications where its magnitude of magnetization is suitable as a cheaper alternative. Examples of potential applications include different kinds of nano-sized magnetic components for eg. Magnetic storage, sensors and data processing. The plausibility of this could be studied with more detailed studies on the matter.

9. Sources

1. Coey, J.M.D.. (2009). *Magnetism and Magnetic Materials*. (pp. 11). Cambridge University Press. Retrieved from <https://app.knovel.com/hotlink/toc/id:kpMMM00003/magnetism-magnetic-materials/magnetism-magnetic-materials>
2. Introduction to magnetic units and types of magnetic ordering (pdf file)
3. SQUID magnetometer manual (pdf file)
4. <https://www.gnu.org/software/octave/about.html>
5. https://en.wikipedia.org/wiki/Magnetic_susceptibility#cite_note-22, original source S. Otake, M. Momiuchi & N. Matsuno (1980). "Temperature Dependence of the Magnetic Susceptibility of Bismuth". *J. Phys. Soc. Jap.* **49** (5): 1824–1828. *Bibcode*:1980JPSJ...49.1824O. *doi*:10.1143/JPSJ.49.1824
6. Cullity, B.D. Graham, C.D. *Introduction to magnetic materials*. Hoboken (NJ): Wiley cop. 2009.

9.1 Image sources

Figure 1, 2, 3,4: Introduction to magnetic units and types of magnetic ordering (pdf file)

Figure 5, 6, 7: SQUID magnetometer manual (pdf file)

Figure 9, 10, 11: Plotted with GNU octave code (see attachment 2)

10. Attachments

1. SamplePlotV2M2PerforatedAndPure.m

```
close all;
```

```
%samples 1 to 3 are perforated
```

```
%samples 4 and 5 are pure
```

```
m1 = 1.360E-2; %masses of samples in grams
```

```
m2 = 1.120E-2;
```

```
m3 = 1.120E-2;
```

```
m4 = 5.180E-2;
```

```
m5 = 8.60E-03;
```

```
m1 = m1*10^-3; %sample masses in kg
```

```
m2 = m2*10^-3;
```

```
m3 = m3*10^-3;
```

```
m4 = m3*10^-3;
```

```
m5 = m3*10^-3;
```

```
%loading measured data into variables. The filenames in dlmread can be changed to load data from different samples/files
```

```
Sample1data = dlmread('TD2_300K80Oe.res')(3:end, 1:end);
```

```
Sample2data = dlmread('TD2_300K_80_Oe.res')(3:end, 1:end);
```

```
Sample3data = dlmread('TD2_300K_80Oe.res')(3:end, 1:end);
```

```
Sample4data = dlmread('perforated_graphite_S1_8p8mg (Pure Graphite) 80 Oe.res')(3:322, 1:end); %remove additional points from the graph
```

```
Sample5data = dlmread('Pure Graphite_RW-A_8p6mg (Italy) 80 Oe.res')(3:end, 1:end);
```

```
Tb1 = Sample1data(1:end,2); %Temperature in kelvins
```

```
Tb2 = Sample2data(1:end,2);
```

```

Tb3 = Sample3data(1:end,2);
Tb4 = Sample4data(1:end,2);
Tb5 = Sample5data(1:end,2);

Z_Moment1 = Sample1data(1:end,4); %Z-moment in A*m^2
Z_Moment2 = Sample2data(1:end,4);
Z_Moment3 = Sample3data(1:end,4);
Z_Moment4 = Sample4data(1:end,4);
Z_Moment5 = Sample5data(1:end,4);

Mmag1 = (Z_Moment1./m1); %mass magnetization in emu/g
Mmag2 = (Z_Moment2./m2);
Mmag3 = (Z_Moment3./m3);
Mmag4 = (Z_Moment4./m4);
Mmag5 = (Z_Moment5./m5);

%Saturation magnetization for inverse magnetization. Approximated from magnetization at T=300K
M01 = -0.0001398;
M02 = -0.0001017;
M03 = -0.0000895;

%Inverse mass magnetization 1/(M-M0). Proportional to inverse susceptibility: 1/chi = H/M

invMmag1 = 1./(Mmag1-M01);
invMmag2 = 1./(Mmag2-M02);
invMmag3 = 1./(Mmag3-M03);

%Curie-Weiss fit: 1/M-M0 = (T-Tc)/C, approximated by guessing values until approximate fit.

FitM1 = (Tb1-(-2))./0.0009;
FitM2 = (Tb2-(-1))./0.0025;
FitM3 = (Tb3-0)./0.0023;

%Plot the graphs
plot(Tb1, Mmag1, 'r*');
hold on
plot(Tb2, Mmag2, 'c*');

```

```

plot(Tb3, Mmag3, 'y*');
plot(Tb4, Mmag4, 'b*');
plot(Tb5, Mmag5, 'g*');
grid on;

%Fitted lines
%plot(Tb1, FitM1, 'r');
%plot(Tb2, FitM2, 'c');
%plot(Tb3, FitM3, 'y');

%Plot metadata
title ("Graphite samples 1, 2, 3 (perforated) and 4 and 5 (pure), H=800e");
xlabel ("T[K]");
ylabel ("M)[emu/g]");
%ylabel ("1/M-M0[g/emu]");
legend ("Sample1 (perforated at 280°C)", "Sample2 (perforated at 800°C)", "Sample3 (perforated at 1000°C)",
"sample4 (pure, S1_8p8mg)", "sample5 (pure, RW-A_8p6mg)");
%legend("Sample1 (perforated at 280°C)", "Sample2 (perforated at 800°C)", "Sample3 (perforated at 1000°C)",
"Line fit 1/M-(-0.0001398) = (T-(-2))/0.0009", "Line fit 1/M-(-0.0001017) = (T-(-1))/0.0025", "Line fit 1/M-(-
0.0000895) = (T-0)/0.0023");

title ("Perforated samples, 1/M(T)");

```

2. SQUID description + Introduction to magnetic units and types of magnetic ordering.pdf

INTRODUCTION

Welcome to the Cryogenic S700X SQUID magnetometer manual for the measurement of magnetic properties as a function of magnetic field and temperature. Superconducting Quantum Interference Device (SQUID) is a highly integrated instrument system, designed to be a primary research tool in the complicated study of magnetism in matter. The magnetic signature of a material reflects its intrinsic spin and orbital angular momentum. In the case of a material that would normally be recognized as strongly magnetic, i.e., the ferromagnets used in electric motors or the material used on magnetic recording tape, determining a "magnetization curve" over a range of applied magnetic fields will help establish its commercial value for a particular application. For other materials, those that might be characterized by most people as "non-magnetic," a similar investigation might reveal information about electronic structure, interactions between neighboring molecules or the character of a transition between two phases of the material.

The SQUID is the most sensitive detector of magnetic flux available and is in principle capable of detecting 10^{-6} flux quanta variations in magnetic flux. Sample temperature can be controlled continuously from 1.6 K to 400 K as standard. Magnetic field is applied using a superconducting magnet with a maximum field of 7 T. The SQUID has several modes of operation. However, only one mode will be used in the measurement (extraction magnetometry), the essence of which is to measure the total magnetic moment by moving the sample through a set of pick-up coils (a scan length can be varied from 2 to 120 mm). All magnetic measurements are performed exclusively in the short-circuit mode of the superconducting solenoid. The magnetic flux in the solenoid circuit is quantized, and the magnitude of the magnetic field assumes strictly fixed values (DC measurements) that is essential for materials, which exhibit magnetic hysteresis. This is a significant advantage of the system, because the coils register a constant magnetic flux so that it is not needed to move the sample with high speed through the pick-up coils.

1. Operation principle

SQUID magnetometer is a sensitive device for converting magnetic flux into electrical signal of DC/AC current, the action of which is based on the phenomenon of magnetic flux quantization in a superconducting ring with Josephson junctions included in it (See Fig. 1).

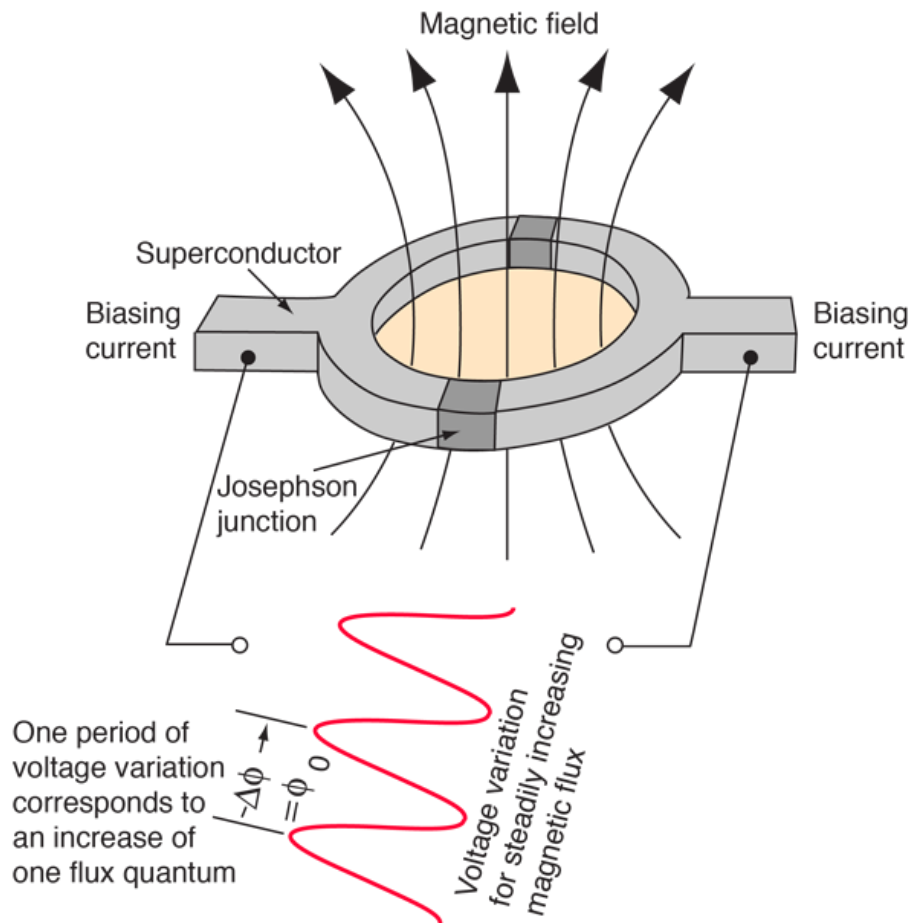


Figure 1. Illustration describing the Josephson effect with two superconducting regions and two Josephson junctions.

We know that electrons possess wave properties. In Josephson ring the electron wave is divided into two, each of them passes through tunnel junction, and then both waves are converged together. In the absence of external field, both branches will be equivalent, and both waves will arrive without any phase difference. However, in the presence of magnetic field, circulating superconducting current will be induced in the circuit. This current will be subtracted from the constant external current in one of the contacts, and will be added in the second contact. Therefore, the two branches will have different currents, and phase difference will appear between the tunnel junctions. Electron waves, passing through the contacts, will interfere. We will see voltage oscillation across the ring, with period Φ_0 , when we steadily increase magnetic flux through the ring (See Fig. 3). The stepwise nature of the dependence makes it possible to distinguish individual flux quanta. In a way, this is analog of the optical effect with interference from two slits, but in this case, currents interfere.

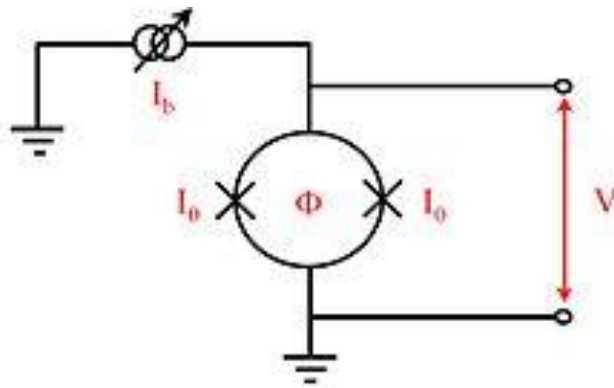


Figure 2. Circuit diagram of DC SQUID magnetometer, where I_b - bias current through the superconducting ring, I_0 - critical current, Φ - magnetic flux applied to the circuit, V - voltage drop.

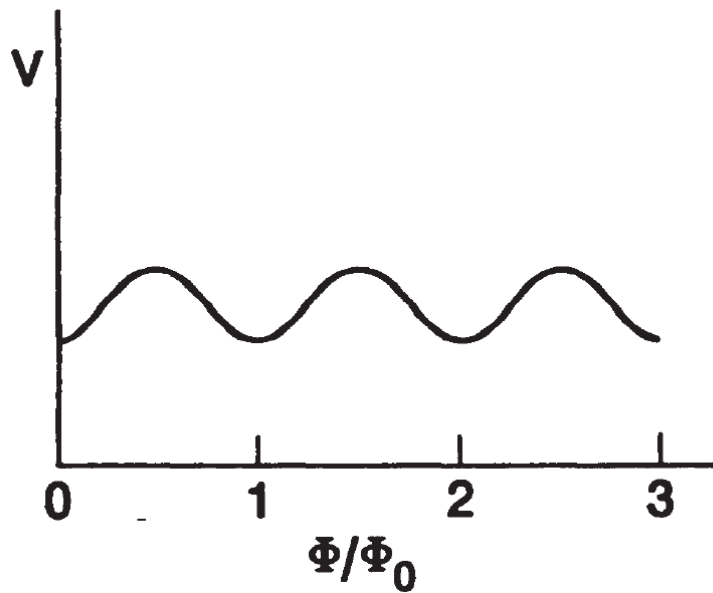


Figure 3. Periodic voltage response due to flux change through a ring. The periodicity is equal to one flux quantum (Φ_0).



Figure 4. Two main parts of SQUID setup: cryostat (on the left) and electronic rack (on the right).

2. Cryostat

The section views of recondensing cryostats is shown on figure 5. The cryostat consists of an aluminum outer shell, containing a helium reservoir, constructed from welded aluminum with a glass fiber/epoxy composite neck and tail section. Ambient magnetic fields (i.e. the Earth's magnetic field) are shielded in the interior of the cryostat to sub μT using a Mu metal shield. Additionally, a niobium can is mounted in the tail section, which, when superconducting, stabilizes any remaining ambient magnetic field that penetrates the Mu metal shield. The base of the helium reservoir tail is fitted with a Carbon Ceramic Sensor (CCS) thermometer and a heater. These are connected to the 6-pin Fischer connector in the cryostat top plate. The temperature response of these thermometers between 300K and 4.2K is calibrated which allows the initial cool-down and subsequent operation of the cryostat to be monitored.

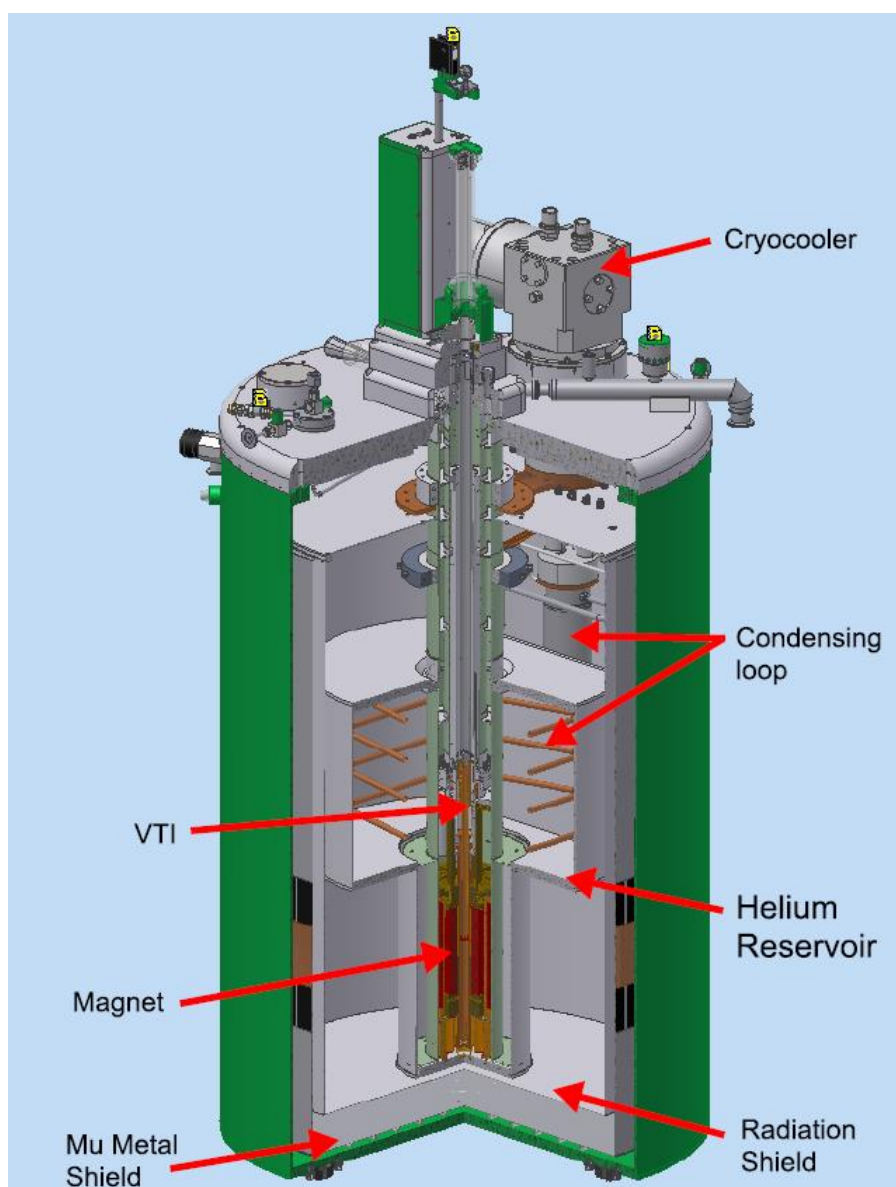


Figure 5. Three quarter section view of the recondensing cryostat and magnetometer insert.

The cryostat contains an arrangement of a helium reservoir and thermal radiation shields in order to improve system performance. The helium reservoir serves to keep the magnets and the SQUID detection circuit in their superconducting state. It also provides the helium for the VTI temperature control system. The helium reservoir volume is 40 L. The amount of liquid helium in the reservoir is determined using a helium level gauge mounted on the Insert. The helium level gauge is connected to the electronics in the rack where it is read in units of mm.

To reduce the rate of helium boil off, there is a shielding system to prevent thermal radiation from the outside reaching the helium reservoir. Constant cooling power comes from the pulse tube cryocooler on the top plate of the cryostat. The first stage of the cryocooler maintains a single radiation shield at 40 K. The second stage, which reaches around 3 K, is used to liquefy a closed loop of helium gas, referred to as the condensing loop. This is separate from the reservoir, but when cold liquid in the condensing loop begins circulate it cools the liquid in the reservoir to below its boiling point of 4.2K and condense the gas.

Magnetometer Insert

The “Insert” (see Figure 6) consists of a **VTI (variable temperature insert)**, **SQUID detector(s)** and **superconducting magnet**. The top of the Insert consists of various levels, which house the connections for the electrical and gas services required to operate the magnetometer.

Superconducting magnet

The superconducting magnet assembly, shown schematically in figure 6, provides a bias field up to 7 Tesla. It features high homogeneity and low drift allowing rapid field change and subsequent field stabilization. The magnet consists of two sections. The “inner” section generates the bulk of the field. It has its own compensation windings to homogenize the field over 4 cm vertical region in the center of the magnet. The “outer” section is a compensation coil to fine-tune the homogeneity of the axial field and to minimize the stray field. The magnet features a “persistent mode” switch that is essentially a non-inductive superconducting connection across the magnet terminals. This forms a closed superconducting loop with the magnet coils and current can flow without loss, meaning the field is persistent without the need for providing a constant current. To change the current in the inductive winding of the magnet, the switch connection must first be driven into the normal (resistive) state. This is accomplished by using a heater at 2 - 3 V from the magnet power supply of the rack. Current from the magnet power supply can then flow through the main inductive section of the magnet and generate the required magnetic field. After the power supply has reached the required current, the persistent switch heater is turned off. This allows the switch to become superconducting again leaving the magnet in persistent mode. The control of the magnet is automated using the LabVIEW software.

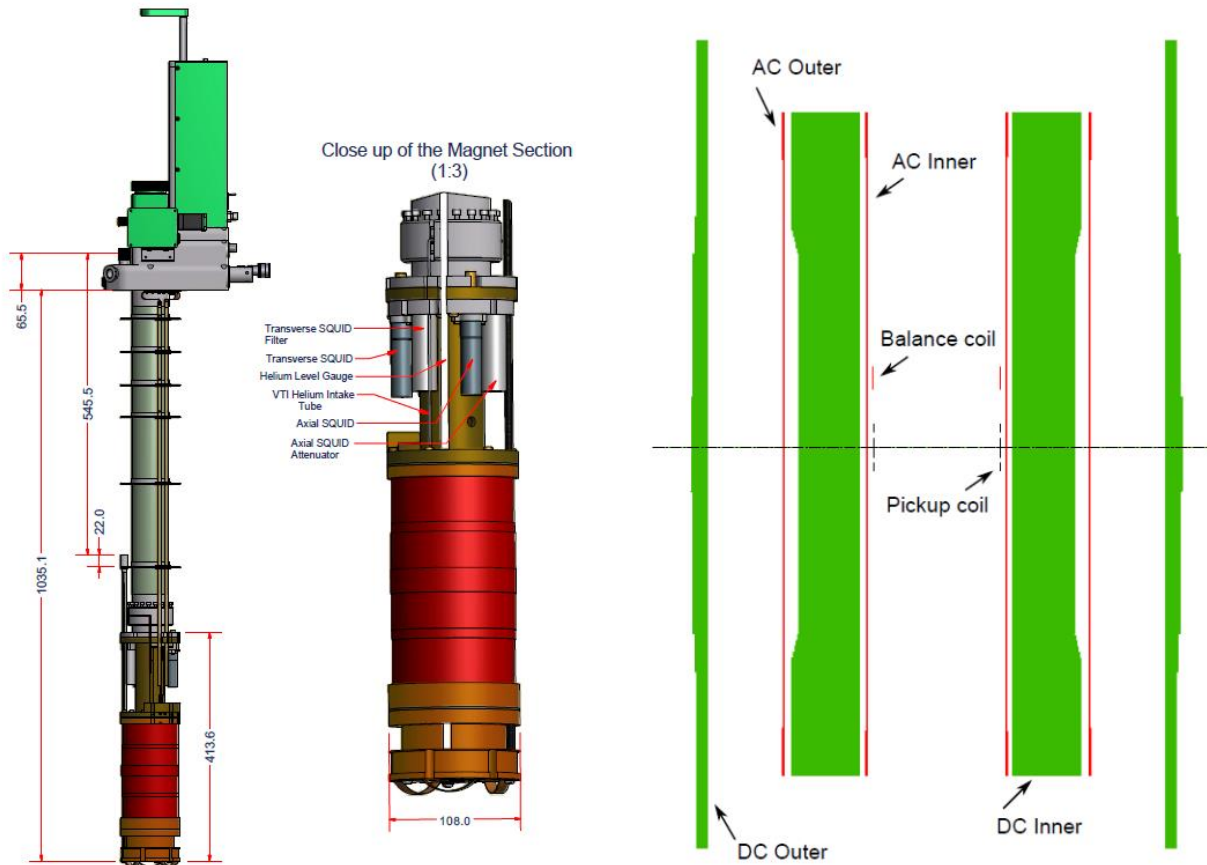


Figure 6. The side view and close up view of the Magnetometer Insert (on the left) and schematic cross-section of the magnet assembly showing the inner and outer sections (on the right).

Superconducting detection coil

The detection coil is a single piece of superconducting wire wound in a set of three coils configured as a second-order (second-derivative) gradiometer. In this configuration, shown in Figure 7, the upper coil is a single turn wound clockwise, the center coil comprises two turns wound counter-clockwise, and the bottom coil is a single turn wound clockwise. The coils are positioned at the center of the superconducting magnet outside the sample chamber such that the magnetic field from the sample couples inductively to the coils when the sample is moved through them. The gradiometer configuration is used to reduce noise in the detection circuit caused by fluctuations in the large magnetic field of the superconducting magnet.

The gradiometer coil set also minimizes background drifts in the SQUID detection system caused by relaxation in the magnetic field of the superconducting magnet. Ideally, if the magnetic field is relaxing uniformly, the flux change in the two-turn center coil will be exactly canceled by the flux change in the single-turn top and bottom coils. On the other hand, the

magnetic moment of a sample can still be measured by moving the sample through the detection coils because the counter wound coil set measures the local changes in magnetic flux density produced by the dipole field of the sample. In this application a second-order gradiometer (with three coils) will provide more noise immunity than a first-order gradiometer (with two coils), but less than a third-order gradiometer (which would employ four coils).

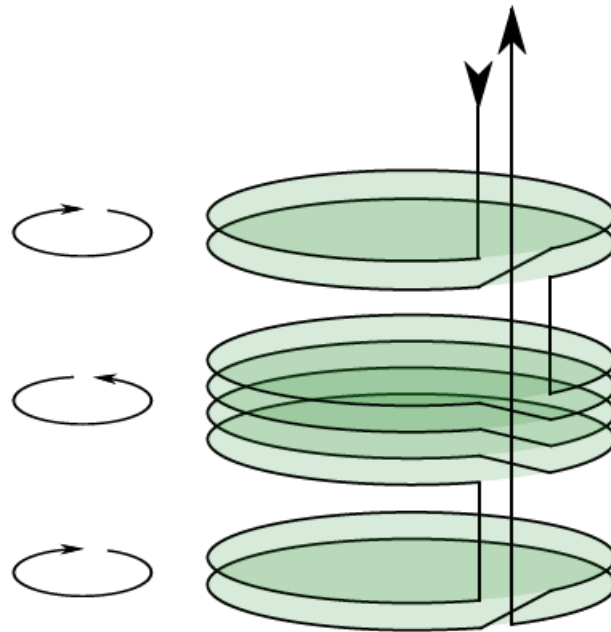


Figure 7. Set of axial pickup coils wound in a second order gradiometer configuration.

It is important to note that small differences in the area of the counter wound coils will produce an imbalance between the different coils, causing the detection coil system to be somewhat sensitive to the magnetic field from the superconducting magnet. In practice, it is never possible to get the coils exactly balanced against the large fields produced by the magnet, so changes in the magnetic field will always produce some current in the detection coil circuit.

Variable Temperature Insert

The inside of variable Temperature Insert (VTI) is composed of two parts: a lower section of thin phosphor bronze tube with a diameter of 9 mm and upper section of stainless steel tube with a diameter of 19 mm. There is a small opening at the bottom of the lower section, which allows helium to flow into the VTI from the needle valve (See Fig. 8). The outside of VTI is composed of a glass fiber tube and a stainless steel / brass tail assembly. The inside of the VTI is thermally isolated from the helium reservoirs by a high vacuum ($\approx 10^{-5}$ mbar).

Temperature control is shown schematically in figure 8. Liquid helium is drawn from the reservoir. It passes through a constriction in the form of a needle valve. The impedance of the valve causes a sharp drop in pressure, which cools the helium by the Joule-Thomson effect. The helium is being vaporized and cooled to around 1.5 K. The cold gas is then passed through a heat exchanger where is warmed to the desired temperature by a heater before being passed through the sample chamber. The sample chamber is made from phosphor bronze, which is a poor electrical conductor, in order to avoid Eddie current heating. This means it is also a poor thermal conductor. The gas flow is laminar due to its low speed resulting in the gas speed being almost zero at the inner surface of the sample chamber. This reduces the thermal exchange between the gas and the sample chamber. To minimize thermal gradients along the length of the chamber, three copper wires (a good thermal conductor) are attached vertically to the outside. To improve heating rates, the chamber is also fitted with a non-inductively wound auxiliary heater, also called film burner. The system is made as adiabatic as possible - so that once the heat capacity of the chamber is overcome and the desired temperature is reached the auxiliary heater can be switched off. The temperature controlled gas flow is then sufficient to maintain the desired temperature. There are two thermometers used for temperature control - thermometer A is located on the heat exchanger and effectively measures the temperature of the gas coming from the heat exchanger to the sample chamber. Thermometer B is positioned in the sample chamber above the sample position. Once equilibrium has been reached, temperature from thermometer B can be taken as the sample temperature.

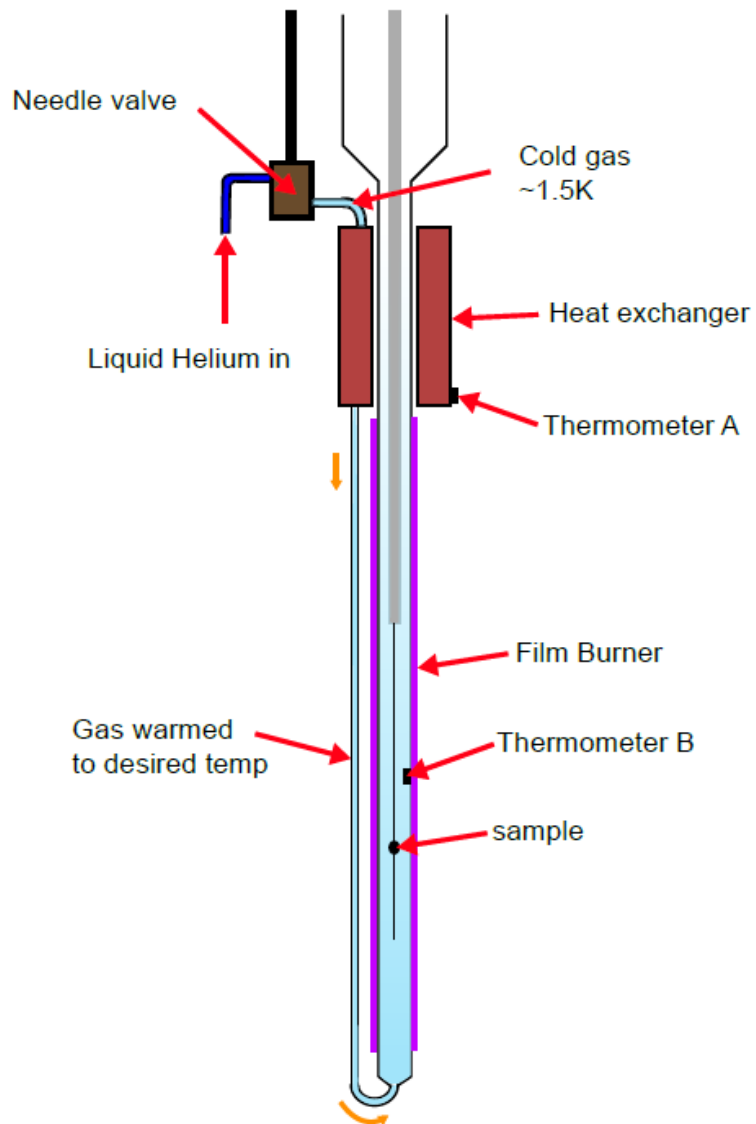


Figure 8. Schematic depiction of the temperature control of sample space.

Stepper motors

A stepper motor (See Fig. 9) moves the sample probe vertically up and down through the pick-up coils. The longitudinal motor makes 16,000 steps per cm. The longitudinal mechanism has three optical switches to act as reference points in case the motor stalls and the software loses the position of the probe. There are upper and lower limit switches at the top and bottom of the full range of the mechanism. When a tag on the motor passes through one of these switches then the software knows where the motor is. The third switch is in the center and is referred to as the home position. By moving to the upper limit and reaching the upper switch then the software knows that the motor is above the home position and it can then move downwards until it finds the home switch.

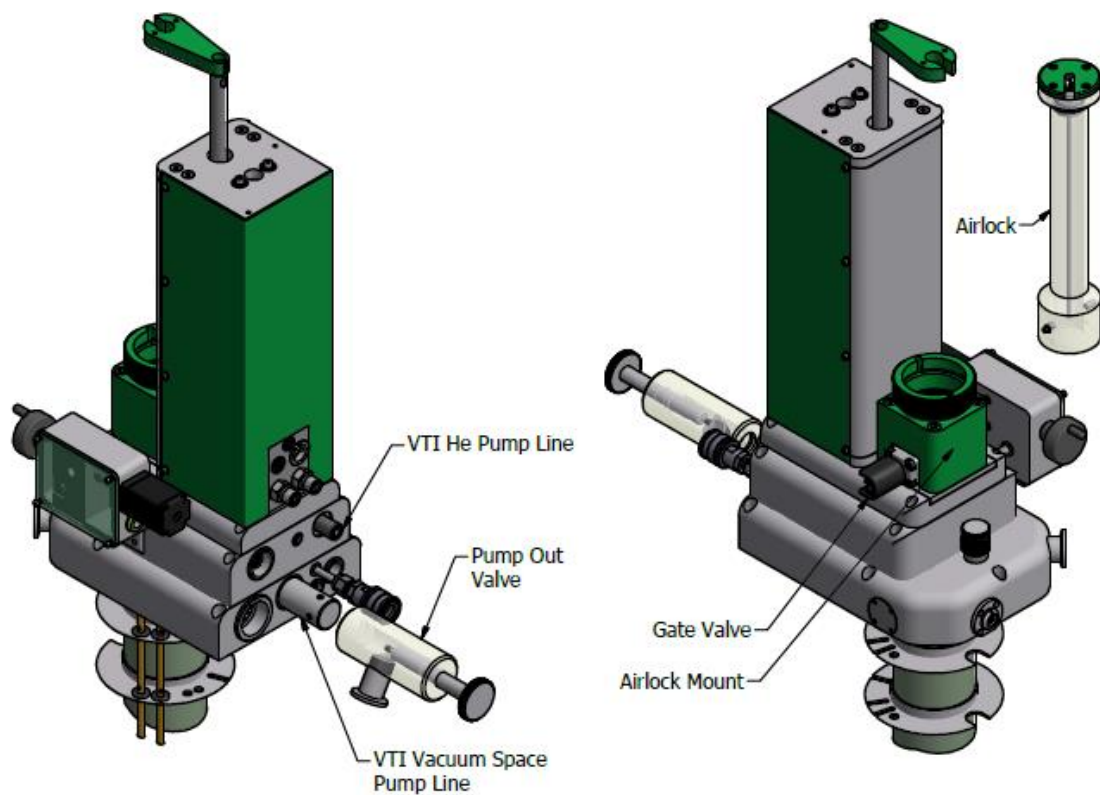


Figure 9. Upper section of the magnet Insert with stepper motor.

3. The electronic rack

The electronic systems are housed in a standard size electronics rack (59.9 cm x 174.0 cm x 80.0 cm). The rack consists of:

LakeShore 218 monitors temperatures of some thermometers located inside the cryostat.

Temperature Controller monitors all thermometers and controls the temperature of the VTI heat exchanger.

Level gauge and DC SQUID interface measure the level of the liquid helium in the reservoir. The SQUID output can be monitored via a BNC connector and displayed on the panel.

Stepper motor panel controls the sample position within the pick-up coils. Front panel LEDs indicate that the motor is activated.

Data acquisition unit (DAQ) / Valve block indicator panel control all analogue and digital inputs and outputs to the system hardware except the magnet power supply and temperature controller. The red LED indicates power to the data acquisition unit and the green LED indicates that computer is properly connected. A schematic diagram of the helium circuit is light with red/green LEDs indicating which valves are closed / open, respectively.

Electronic filter unit houses the electronic filtering circuits for all electrical services connected to the insert, the power supplies for the VTI heaters and SQUID / magnet detection circuit.

Computer runs the S700X software and controls the various electronic systems.

Superconducting magnet power panel controls the current in the superconducting magnet.

Valve block module contains the electronically controlled valves that operate gas systems as well as a pressure gauge for the VTI.

References

1. Cryogenic Limited. S700x squid magnetometer, user manual. pages 1–199, 2017.
2. McElfresh M. Fundamentals of magnetism and magnetic measurements. Quantum Design. 1994.

This section is meant to serve both as an introduction and as a reference section on magnetic units. The units of magnetism are complicated by the fact that over the years they have been defined in several different ways. There has been a great deal of reluctance for parts of the magnetics community to convert to SI units. SI stands for *Système Internationale d'Unités*, which are the official units of measure agreed upon by most nations. However, the most common system of units used among physicists, for reporting magnetic measurement results, is the Gaussian cgs system, which stands for "centimeter, gram, second." To add to the complexity, most physical properties can be reported in a variety of ways. For example, even in cgs units, the magnetization might be given in emu/g, emu/cm³, emu/mole, emu/atom, or any one of several other possibilities. Here, emu stands for *electromagnetic units*.

We must first choose a definition for the different "fields" involved. We can define three fields:

H, the applied magnetic field,

M, the magnetization, and

B, the flux density.

In cgs Gaussian units, the different fields are related by the equation

$$B = H + 4\pi M. \quad (1)$$

In our chosen definition, H is the field applied by the superconducting magnet residing outside of the sample space. This field is determined by the electric currents running in the magnet and, by our definition, it does not change when we place our sample into the magnet.

One way to look at the definition in Eq. 1 is to think of B as the net local field, H is the field from the magnet, and M is the field which changes the local field from H to B. The MPMS moves the sample through the pickup coils in order to change B within the pickup coil, and thereby changes the current flowing in the pickup coils. The amount of current induced is related to the total *magnetic moment* of the sample.

The units of magnetic moment are emu (in cgs) and A·m² (in SI units, where A is amperes and m is meters). The MPMS reports values of magnetic moment in emu. We get the magnetization M by dividing the value of the magnetic moment by volume, mass, or the number of moles in the sample.

The units for B are gauss (denoted G), in cgs units, and tesla (denoted T), in SI units. There is 1 G in 10⁻⁴ T. The units for H are oersted (denoted Oe) in cgs units, and A/m in SI units. An Oersted and a Gauss have the same dimensions, and gauss

is often used for both B and H in conversation. There is 1 Oe in $1000/4\pi$ A/m. From Eq. 1 we expect that M might also be reported in units of G. It is the volume magnetization, which is the magnetic moment of the sample divided by its volume (emu/cm^3), that can be reported in units of G. There is 1 emu/cm^3 in 1000 A/m and there is 1 emu/cm^3 in 4π G. We may also report M in units of emu/g , by dividing the magnetic moment by the mass of the sample in grams, or in emu/mole , by dividing the moment by the number of moles. Sometimes it is the magnetism associated with a certain atom in the compound that is to be measured, in which case we might report, for example, $\text{emu}/\text{Cu-atom}$ where we divided the moment measured by the number of moles of Cu atoms in the sample (similar units exist in the SI unit system). A very useful table of units and conversions, compiled by R. B. Goldfarb and F. R. Fickett of the National Institute of Standards and Technology in Boulder, Colorado, is included as Appendix A.

Two other quantities frequently used in magnetism are the magnetic susceptibility and the permeability. The susceptibility is given by $\chi = M/H$ and the permeability by $\mu = B/H$. These quantities are often used incorrectly. If an M(H) curve is not linear (a straight line), χ will depend on the value of H. Some do not consider an H-dependent χ value to be a legitimate quantity. However, whenever an H-dependent χ is to be reported, it is important that the H value associated with the χ measurement be included. The proper use of these quantities will be discussed further in later sections.

Every material exhibits some kind of magnetic behavior. However, the term “magnetic” is usually used to refer to something that will attract a piece of iron or a permanent magnet. This is a particular type of magnetism called *ferromagnetism* and is only one of the many types of magnetism. We use a magnetometer to measure the magnetization (amount of magnetism) of a sample. By studying how the magnetization changes with temperature and how it changes with the size of the magnetic field we apply to the sample, we can determine the type of magnetism and important related parameters.

There are two principal magnetic measurements:

$M(H)$ - magnetization as a function of applied magnetic field, and

$M(T)$ - magnetization as a function of temperature.

Here, H is the *applied magnetic field* which is the magnetic field applied to the sample by the superconducting magnet coil. An $M(H)$ measurement is made by fixing the temperature T and measuring M at a series of H values. An $M(T)$ measurement is made by fixing the applied field H and measuring M at a series of T values. There are other less common measurements, like magnetization as a function of time $M(t)$, that will also be discussed later. There are many different origins for the magnetic behavior observed in materials, and $M(H)$ and $M(T)$ measurements provide valuable information about the different possible types of magnetic behavior.

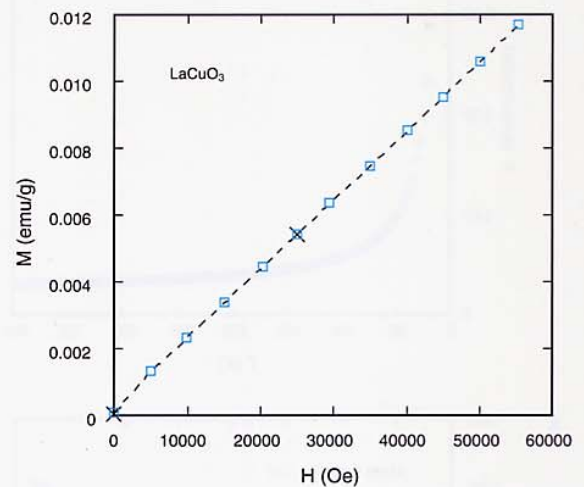
A. PARAMAGNETISM

INTRODUCTION

Probably the simplest type of magnetic behavior is known as *paramagnetism*. Shown in Figure 6 is a plot of $M(H)$ for a typical paramagnet at a fixed temperature. The key features are that 1) the curve is linear, 2) the line intersects zero, and 3) the magnetization is *reversible*. Reversible means that the same curve is followed when going up in field as when going back down in field. When the $M(H)$ curve is linear, the *magnetic susceptibility* χ , which is given by $\chi = M/H$, is often an important property.

A. PARAMAGNETISM

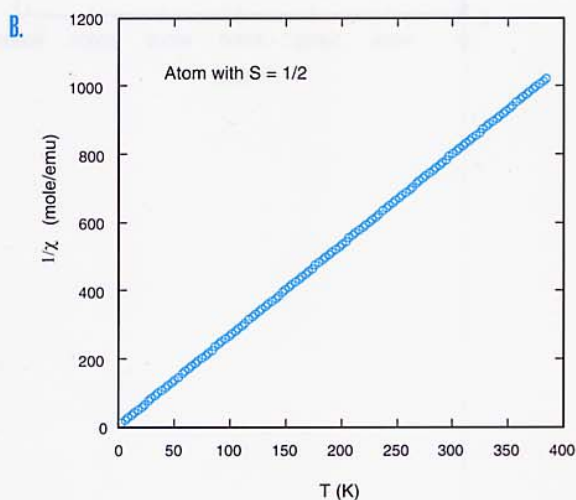
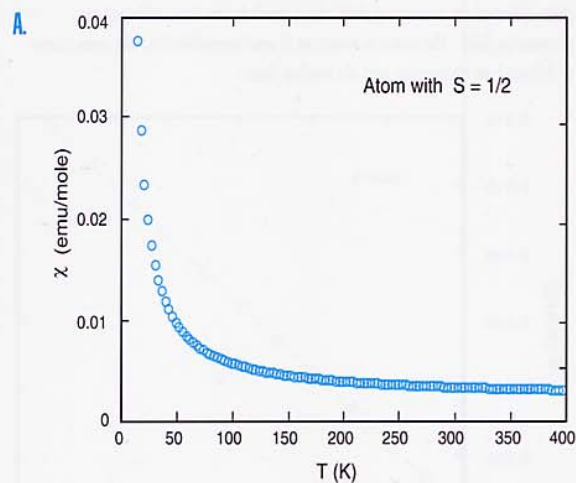
6 Magnetization (M) as function of applied magnetic field (H) for a paramagnetic compound, LaCuO_3 , at $T=100\text{ K}$. The squares are data collected on increasing field, the x -symbols are data collected on decreasing field. The curve is linear in H and reversible (i.e., the same curve is followed on increasing and decreasing field.)



A. PARAMAGNETISM

7

A) Magnetic susceptibility (χ) as a function of temperature (T) for a hypothetical material with nearly ideal Curie paramagnetic behavior having a mole of $S=1/2$ atoms. B) The inverse of χ (in mole/emu) as a function of T . The slope of the curve is proportional to $1/C$.



Curie-Type Paramagnetism

Paramagnetism can have many different origins. Since the $M(H)$ curves are linear, two features are often used to determine the origin of the paramagnetism: the magnitude of χ and the temperature dependence of the susceptibility $\chi(T)$. Shown in Figure 7a is a plot of $\chi(T)$ for a Curie-type paramagnet, which is a type of magnetism resulting from the presence of atoms with unpaired electrons. Curie-type paramagnetism has a particular temperature dependence $\chi(T) = C/T$, where C is a constant. A plot of $1/\chi$ versus T , as shown in Figure 7b, is very useful for characterizing Curie paramagnets. The slope of the curve is equal to $1/C$ and the Curie constant is given as

$$C = b \mu_{\text{eff}}^2 N,$$

where μ_{eff} is known as the *effective magnetic moment*, b is a universal constant, and N is the concentration of magnetic atoms with that moment. Thus, the constant C can be used to determine the *product* of the effective magnetic moment of an atom and the number of magnetic atoms present. If the number of magnetic atoms is known (from a mass measurement, for example), it is then possible to determine μ_{eff} associated with the magnetic atom.

UNITS

When $M(H)$ is linear and reversible it is possible to define the magnetic susceptibility as $\chi = M/H$. The MPMS reports the magnetic moment m in units of emu, a cgs unit. If this is divided by the volume (in cm^3) one will have the volume magnetization M (in emu/cm^3). Dividing this M by the applied field H (in Oe) gives the volume susceptibility, which is dimensionless, but often expressed as emu/cm^3 or $\text{emu}/(\text{cm}^3 \text{ Oe})$. Similarly dividing m by the mass in grams (g) gives the mass magnetization M_g (or σ). Dividing M_g by H in Oe gives the mass susceptibility, which is expressed as emu/g . Dividing m by the number of moles gives the molar magnetization M_m in emu/mole . Dividing this by H in Oe gives the molar susceptibility, which is also expressed as emu/mole . These can be converted to SI units using the table in Appendix A.

EXAMPLES AND ADVANCED TOPICS

Curie Paramagnetism

To determine the μ_{eff} for a Curie-paramagnetic sample will first require calculating the molar susceptibility values (often denoted χ_m). Next $1/\chi_m$ is plotted as a function of temperature, like the data shown in Figure 7b. If the $M(H)$ curves are linear, the χ_m value at any magnetic field can be used. For a Curie paramagnet the $1/\chi_m$ curve will intercept zero and have a slope $1/C_m$, where C_m is the molar Curie

units of emu-K/mole. To get p_{eff} from C_m , we use the complete formula

$$C_m = (N p_{\text{eff}}^2) / 3 k,$$

where N is Avogadro's number (6.02×10^{23}) and k is Boltzmann's constant (1.38×10^{-16} erg/K). Rearranging this gives

$$p_{\text{eff}} = (3 k C_m / N)^{1/2},$$

with p_{eff} in units of erg/Oe. The effective moment is usually reported in units of Bohr magnetons (denoted μ_B). Dividing by 0.927×10^{-20} (erg/Oe)/ μ_B will give p_{eff} in units of μ_B . A shortcut to getting p_{eff} (in μ_B) from C_m (in emu K/mole) is to use

$$p_{\text{eff}} = 2.82 C_m^{1/2}. \quad (2)$$

The χ data in Figure 7b are in units of emu/mole. The slope of this curve is 2.66 and since the slope equals $1/C_m$, this gives $C_m = 0.376$. Using Eq. 2 we find that $p_{\text{eff}} = 1.73 \mu_B$, which is the effective moment associated with spin $s = 1/2$ atoms like those of Cu^{2+} .



OTHER TYPES OF PARAMAGNETISM

Curie-Weiss Paramagnetism

For a Curie-type paramagnet, there is a force that tries to align the magnetic moments on atoms with the magnetic field ($p_{\text{eff}} \cdot \mathbf{H}$). The $1/T$ (or Curie) temperature dependence is a result of a competition between the force aligning the moments parallel to the field and the tendency for heat to disrupt the alignment. As the temperature increases, the associated increase in heat reduces the relative effect of the field.

What is different about a *Curie-Weiss* paramagnet is that, in addition to the interaction with the applied magnetic field, there is an interaction between the magnetic moments on different atoms. This interaction between moments (exchange interaction) can help align adjacent moments in the same direction or it can help align neighboring moments in opposite directions.

The Curie-Weiss susceptibility is given by

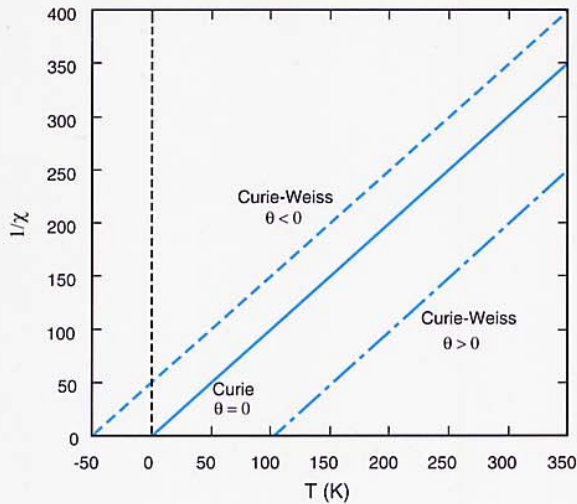
$$\chi_{\text{CW}} = C/(T - \theta), \quad (3)$$

where θ is called the *Curie-Weiss temperature*. The Curie-Weiss θ is related to the strength of the interaction between moments, and its sign depends on whether the interaction helps align adjacent moments in the same direction or opposite one another. Using the definition in Eq. 3, for $\theta > 0$ the interaction helps to align adjacent moments in the same direction, and for $\theta < 0$ the interaction helps to align adjacent moments opposite each other. Other terminology, which will become

B. DIAMAGNETISM

8

The inverse of χ as a function of T for systems exhibiting Curie ($\chi = C/T$) and Curie-Weiss behavior ($\chi = C/(T-\theta)$). When $\theta > 0$ the interaction between moments helps to align neighboring moments in the same direction and when $\theta < 0$ moments are aligned in opposite directions. When $\theta = 0$ the moments act completely independent of one another.



clearer in later sections, is that for $\theta > 0$ there is a net *ferromagnetic interaction* between moments and for $\theta < 0$, there is a net *antiferromagnetic interaction* between moments.

The characteristic plot for Curie behavior was the $1/\chi$ versus T plot, and the same is true for Curie-Weiss behavior. But as shown in Figure 8, instead of a straight line through zero, as in Figure 7b, we get an x-axis intercept at a positive or negative θ . In the case of the ferromagnetic θ ($\theta > 0$), it can be seen that Eq. 3 diverges (goes to infinity) at $T = \theta$. This is the approximate location of a ferromagnetic transition, also known as the *Curie temperature* (denoted T_C). For an antiferromagnetic θ ($\theta < 0$), Eq. 3 will not diverge at $T = \theta$. However, the system may now have an antiferromagnetic transition, known as a Néel transition (denoted T_N), near $T = |\theta|$.

Pauli Paramagnetism and Van Vleck Paramagnetism

Pauli paramagnetism is observed in metals and is due to the fact that conduction electrons have magnetic moments that can be aligned with an applied field. The key characteristics of Pauli paramagnetism are that the χ value is nearly independent of temperature and in most cases it has a very small value.

Van Vleck paramagnetism is another type of paramagnetism that is also nearly independent of temperature and usually has a small value. Van Vleck paramagnetism is associated with thermal excitations to low-lying states.

Combinations

Often the temperature dependence of the paramagnetism does not follow any particular dependence. In these cases it can be useful to see if the behavior can be fit by an equation that combines a temperature independent part and a Curie, or Curie-Weiss, part. Antiferromagnets also have $M(H)$ curves like paramagnets, even below T_N . The $M(T)$ behavior is distinctive for well-behaved antiferromagnets, and is confusing in other cases. Antiferromagnetism will be discussed in more detail below.

There are also a variety of much more complicated magnetic behaviors that are active areas of research and are not easily identified by an $M(T)$ curve. These include heavy-fermion systems, mixed-valence systems, spin-density-wave systems, spin glass systems, as well as others.

B. DIAMAGNETISM

When an $M(H)$ plot is linear and reversible but has a negative slope, we describe the magnetic behavior as diamagnetism. This means that χ is negative. In most cases a diamagnetic contribution to the magnetism arises from paired electrons and the value of this contribution is usually extremely small. Tables of the contributions

due to certain atoms and atom combinations, usually called *Pascal's Constant tables*, are used for approximating these contributions. The other important type of diamagnetism is superconductivity, which can have the largest possible value of diamagnetism. This will be discussed at length below.

There is an interesting observation one can make about diamagnets: they are repelled by a magnetic field. On the other hand, a paramagnet is attracted into a magnetic field. A simple picture for this is to think of the magnetic field to be composed of lines of magnetic field. The density of lines at any point is proportional to the field B . A diamagnet will push field lines out while a paramagnet will pull them in. Thus, for a diamagnet $B < H$ inside the sample and for a paramagnet $B > H$ inside the sample.

C. FERROMAGNETISM

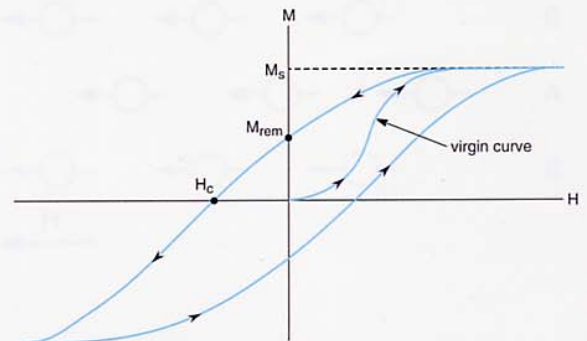
INTRODUCTION

Ferromagnetism is a very important type of magnetism. Ferromagnets, and the related ferrimagnets, are the materials we usually call magnets - they are attracted to a piece of iron or a permanent magnet. The strongest type of magnetism found in materials is ferromagnetism. Ferromagnets have very distinctive $M(H)$ and $M(T)$ curves. Figure 9 shows a typical $M(H)$ curve for a ferromagnet at a fixed temperature. The key features are that the curve is *not* linear and the behavior is *not* reversible. The lack of reversibility is often called *magnetic hysteresis*. Figure 9 shows that as H is increased the magnetization gradually reaches a maximum value known as the *saturation magnetization*, which is usually denoted M_s . The saturation magnetization is an important property of a ferromagnet that is the same for any piece of a particular compound (it is an *intrinsic property*) no matter what the material's processing history has been.

As H is reduced back to zero from saturation, we can see in Figure 9, that a different curve is followed on the way down and that M does not go to zero when H returns to zero. The value of the *magnetization* when H is returned to zero is called the *remanent magnetization*, denoted M_{rem} . The remanent magnetization is often confused with the saturation magnetization, but they are very different properties. Whereas the saturation magnetization is an intrinsic property of a compound, the remanent magnetization depends on the way a sample of the material has been prepared and treated (its history). A large remanent magnetization is desirable for applications like magnetic recording, whereas a small remanent magnetization is desirable for applications like magnetic transformer cores. Materials with large remanent magnetizations are called *hard ferromagnets*, and those with small remanent magnetizations are called *soft ferromagnets*.



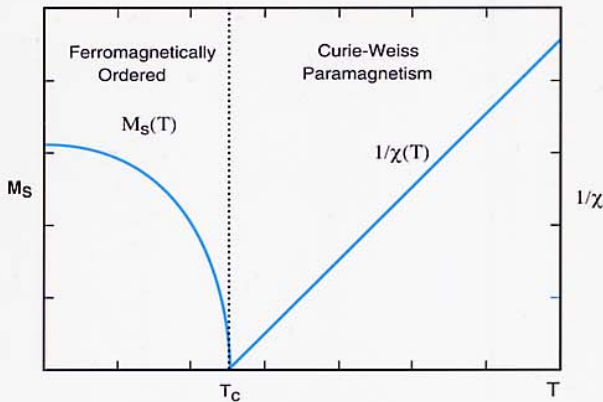
9 Magnetization as a function of field at $T < T_C$, after cooling the sample from above T_C . Identified are the initial magnetization curve (or virgin curve), the saturation magnetization (M_s), the remanent magnetization (M_{rem}), and the coercive field (H_c).



C. FERROMAGNETISM

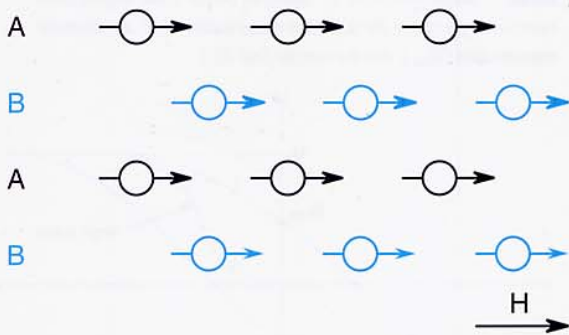
10

Above the Curie temperature (T_C) a ferromagnet is paramagnetic exhibiting Curie-Weiss behavior ($\chi = C/(T-\theta)$) with $\theta > 0$. Below T_C , χ is no longer a useful parameter since χ is both field and history dependent. Instead, the saturation magnetization M_s is an important intrinsic property.



11

Schematic diagram showing how the atomic moments in a ferromagnet are locked together and aligned in the same direction below T_C .



The magnetization of a ferromagnet does not return to zero by reducing H to zero. However, by applying a sufficiently large magnetic field in the opposite direction, the magnetization can be returned to zero. The magnetic field required to return the magnetization to zero is called the *coercive field*, usually denoted H_C . The coercive field is not an intrinsic property and the value of H_C has an additional dependence on the rate of change of the magnetic field dH/dt . The size of the coercive field determines how useful the material is for various applications. Although H_C is related to the remanent magnetization (i.e., if M_{rem} were zero, H_C would also be zero), it is a different property.

So far the description of a ferromagnet has been an operational one. A major distinction between ferromagnets and paramagnets is that the ferromagnetic state is a state of *long range order*. This long range order sets in at a phase transition which occurs at the Curie temperature. The Curie temperature is close to the same point where a $1/\chi$ versus T plot will extrapolate to zero for a Curie-Weiss paramagnet that becomes ferromagnetic. An example is shown in Figure 10 where Curie-Weiss paramagnetic behavior ($\chi = C/(T-\theta)$) with $\theta > 0$ is observed above the transition, while below T_C the system is ferromagnetically ordered. Below T_C , χ is no longer a useful parameter, since χ is both field and history dependent, and instead, it is the saturation magnetization M_s that is an important intrinsic property.

In a ferromagnet below T_C , the individual magnetic moments of the atoms are all lined up in the same direction and essentially locked together as shown schematically in Figure 11. Instead of the magnetic moments acting individually, they act together like one very large magnetic moment. The term "long range order" means that if we know the orientation of one moment at a particular position, we can determine the orientation of any other moment a long distance away. For a ferromagnet, all of the moments within a domain are aligned in the same direction. On the other hand, for a paramagnet the orientation of any moment is random and even though there is a higher probability for a moment to align with the magnetic field, each moment acts nearly independently of the others.

UNITS

The units for magnetization and applied magnetic field are the same for ferromagnets as they are for all types of magnetic systems. It is important to remember that M_{rem} and M_s have values of magnetization, while H_C is a value of the applied magnetic field.

EXAMPLES AND ADVANCED TOPICS

History Dependence

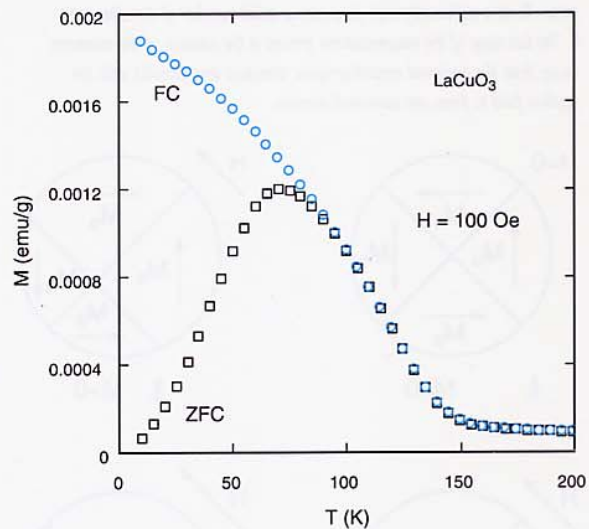
Ferromagnets usually exhibit some amount of irreversibility (or hysteresis) in their $M(H)$ behavior. This irreversibility in the $M(H)$ curves is a part of a more general type of behavior often referred to as *history dependent* behavior. Here, history dependent means that the value of the magnetic moment observed is dependent on the sequence of magnetic field changes and temperature changes that were involved in getting the sample to the condition in which it was measured. In addition to the hysteresis in $M(H)$ curves at fixed temperature, $M(T)$ behavior can also show a dependence on the magnetic field history if M is not saturated on every half-cycle of a $M(H)$ loop.

One way of determining if irreversibility exists is to do a *zero-field-cooled/field-cooled* (ZFC/FC) set of measurements. This is done by cooling the sample to the lowest measurement temperature in $H = 0$. Once stabilized, a magnetic field is applied and the moment is measured as a function of temperature up to the highest desired temperature. This is the ZFC part. Next the sample is cooled in this same field to the lowest temperature and again measured as a function of temperature. This FC part can also be done by collecting data as the sample is cooled, however, most cryogenic systems are more time efficient when collecting on warming. At least in the case of superconductors, the FC data should be collected on cooling, not on warming. This ZFC/FC method is very useful for determining the temperature range over which systems are irreversible. Results of a ZFC/FC measurement are shown in Figure 12.

Another important result of irreversibility in ferromagnets is that the shape of an $M(H)$ curve will change unless saturation is attained on every half cycle of a hysteresis loop. If a magnetic field below saturation is used, a different $M(H)$ curve will be traced. These other curves are usually called *minor loops*. Running a magnetic material through a series of minor loops of decreasing size (smaller and smaller peak values of H) is a method for “demagnetizing” a ferromagnet. Demagnetization can be a misleading term because the sample is still ferromagnetic. When demagnetized, a ferromagnet consists of many small domains within which magnetic moments point in the same direction. Adjacent domains however, have their magnetization pointing in different directions. In this way, the magnetic field lines can close inside the sample and the remanent magnetization is zero. Domains are discussed in the next section.

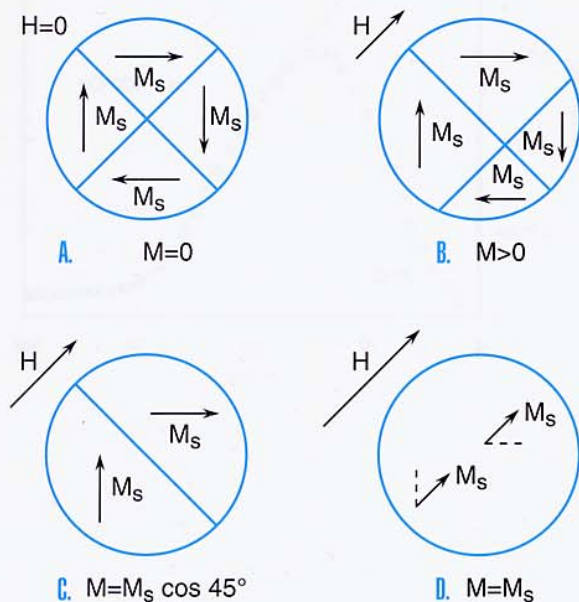
12

Magnetization as a function of temperature for the cases where a) the sample is first cooled in $H = 0$, a field turned on, and then data collected on warming (ZFC) and, b) when data are collected as the sample is cooled in the same field (FC).



13

The magnetization process for a ferromagnetic sample that was cooled from above its T_C . **A.** In $H = 0$ the magnetic domains form a closed loop with the moments aligned along preferred crystallographic directions. Within each domain the magnetization is saturated. **B.** As H is applied the domain walls move to allow the domains aligned with the field to grow. **C.** At a sufficiently high field only a small number of domains exist. **D.** The last stage of the magnetization process is the rotation of the moments away from the preferred crystallographic direction and parallel with the applied field to form one saturated domain.



Magnetic Domains

When a ferromagnet is cooled from a temperature above its Curie temperature in $H = 0$, it will usually show very little evidence of having a large magnetization value. This is due to *domain* formation. Instead of all the magnetic moments in the sample lining up in the same direction in one single domain, the lower energy configuration is for the sample to be divided up into several or many magnetic domains. Within a domain, all of the moments are aligned in the same direction (the magnetization is saturated within a domain). It is important to note that the magnetic domains are not the same as crystallographic domains—the magnetic domains cannot be seen without magnetic imaging techniques. In the border region between different magnetic domains, the direction of the magnetization changes. This border region is called the *domain wall*. It is the way that domain walls move that causes much of the irreversibility in ferromagnets.

When a magnetic field is applied to a sample that has been cooled in $H = 0$ from above T_C , the sample will initially seem to be nonmagnetic. As a magnetic field is initially applied, the $M(H)$ behavior looks like the initial curve identified in Figure 9. This is called the “virgin curve” and the behavior associated with this curve is shown in Figure 13. Initially, the domains are directed so that the spontaneous magnetic fields form a closed magnetic loop. When a magnetic field is applied, more of the moments start to align with the field. This does not happen randomly within all domains, but rather the domains with a component directed along the field direction preferentially grow in size. In Figure 13 this is pictured as the domain wall moving. This selective domain growth continues until the whole sample is one domain. Even though the moments in a domain are parallel to each other, they still may not be aligned with the magnetic field but along some preferred crystallographic direction. This is due to *magnetic anisotropy*, which is a topic for a separate discussion. To reach full saturation requires that the moments turn from their preferred crystallographic direction to be parallel to the magnetic field.

As the field is reduced from saturation, the moments will first return to the preferred crystallographic direction. As the field is decreased further, the domain walls will reform (or nucleate) and try to move. The domain wall motion can, however, be strongly impeded as in the case of hard ferromagnets. This impedance to domain wall motion is caused by domain wall *pinning*. Domain walls can get stuck at various defects, like grain boundaries and inclusions, producing the characteristics of remanence and coercivity.

D. ANTIFERROMAGNETISM AND FERRIMAGNETISM

Magnetic Recording and Transformer Coils

The area within an $M(H)$ loop is the energy dissipated on cycling that sample through the loop. The magnetic cores of ac powerline transformers, which are cycled through an $M(H)$ loop at 50 to 60 times per second, is an example in which a soft ferromagnet is very useful. A large mutual inductance is possible with a minimum of *hysteretic loss*.

An important application of hard ferromagnetic materials is their use in magnetic recording media. Two states are required to store binary data. The recording head is a small magnetic pickup coil that can discern regions having either of the two different directions of magnetization. The head is also used to write these regions. To write, the coil applies a magnetic field, larger than H_c , to the recording media in one or the other direction for a short time. A patch of magnetic material is thereby "switched" into a particular direction. The coercive field (H_c) determines the size of the field necessary to switch the field in that region. On the other hand it is the remanent magnetization (M_{rem}) of the magnetic media that determines how large a magnetization is available for the head to read.

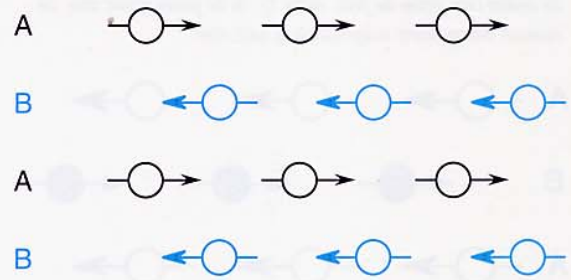
D. ANTIFERROMAGNETISM AND FERRIMAGNETISM

ANTIFERROMAGNETISM

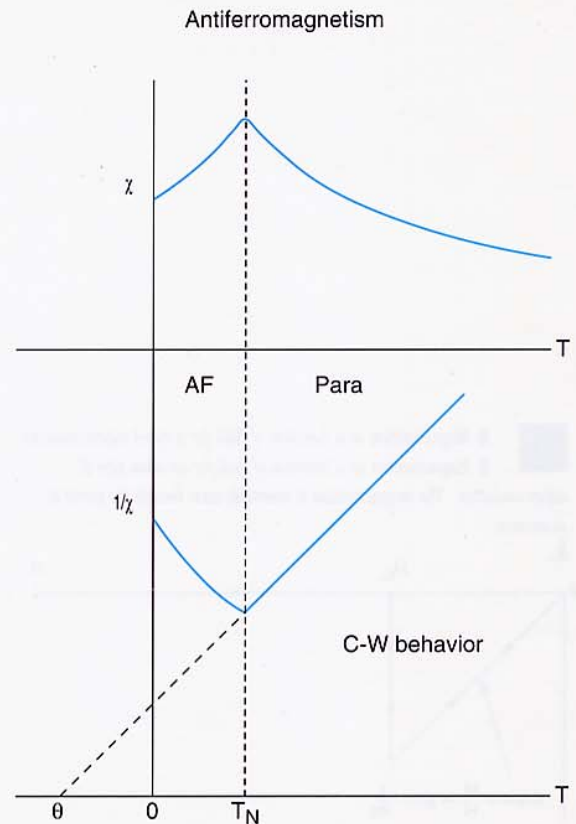
The term *antiferromagnet* often produces considerable confusion. Some people may think that an antiferromagnet is a ferromagnet but with the magnetic moments all lined up opposed to the applied field direction. However, this kind of behavior has never been observed. In an antiferromagnet the magnetic moments line up so that adjacent moments are aligned in opposite directions to each other (see Figure 14). Instead of the enormous combined moments associated with ferromagnets, the moments on neighboring atoms cancel each other, resulting in relatively small values of M . The $M(H)$ behavior is more characteristic of a paramagnet; however, the origin of the $M(H)$ behavior in antiferromagnets is quite different from that of Curie paramagnets, since the antiferromagnetic state is a long range ordered state. The moments are locked together but in the alternating configuration shown in Figure 14.

The temperature dependence of an antiferromagnet is shown in Figure 15. The phase transition to the antiferromagnetic state is known as a Néel transition and occurs at a temperature usually denoted T_N . Above T_N an antiferromagnet is often paramagnetic exhibiting Curie-Weiss behavior ($\chi = C/(T - \theta)$) with $\theta < 0$. Since $M(H)$ curves are linear below T_N , χ remains a useful property.

14 Schematic diagram showing how the atomic moments in an antiferromagnet are locked together and aligned so that adjacent moments have spins in opposite directions. Above T_N , in the paramagnetic state, the moments behave nearly independently of one another.

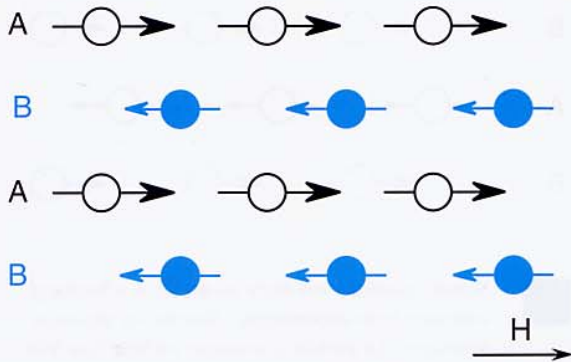


15 Magnetic susceptibility and inverse susceptibility as a function of temperature for an antiferromagnet. Above the Néel temperature (T_N) a antiferromagnet often resembles a paramagnet exhibiting Curie-Weiss behavior ($\chi = C/(T - \theta)$) with $\theta < 0$.

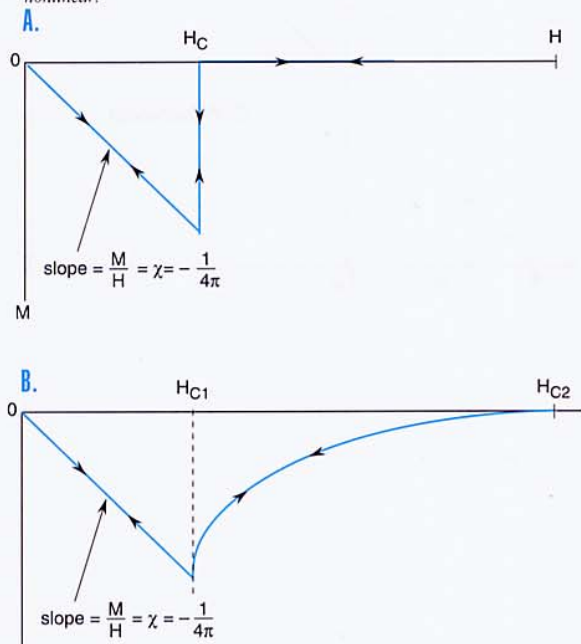


E. SUPERCONDUCTIVITY

16 Schematic diagram showing how the atomic moments in a ferrimagnet are locked together and aligned so that adjacent moments have spins in opposite directions. The adjacent moments are of different size. The larger moments usually line up with the applied field and the smaller ones oppose the field. Above T_C , in the paramagnetic state, the moments behave nearly independently of each other.



17 A) Magnetization as a function of field for a type-I superconductor. B) Magnetization as a function of field for an ideal type-II superconductor. The magnetization is reversible even though the curve is nonlinear.



FERRIMAGNETISM

Ferrimagnets are often associated with ferromagnets because their $M(H)$ and $M(T)$ behavior is nearly identical to that of ferromagnets. However, at the atomic level ferrimagnets are more similar to antiferromagnetics because the magnetic moments of the atoms in ferrimagnets are antiferromagnetically coupled; i.e., adjacent magnetic moments are locked in opposite directions. What makes ferrimagnets different from antiferromagnets is that the adjacent moments have different magnitudes. The larger of the two moments tends to align with the applied magnetic field while the smaller moment aligns opposite to the field direction (see Figure 16). The result is that the different moments add up to produce a large net moment aligned with the magnetic field. Some of the most useful materials for making permanent magnets are ferrimagnets. Many of these materials are non-electrically conducting ceramics.

UNITS

Antiferromagnets behave essentially like paramagnets. On the other hand, ferrimagnets behave essentially like ferromagnets, having the same types of irreversibility possible and the same parameters (H_C , M_{rem} , and M_S) used to describe their behavior.

E. SUPERCONDUCTIVITY

INTRODUCTION

Another very important type of magnetism is associated with superconductivity. The magnetic properties of superconductors are unique and very complex. Figure 17a is a plot of $M(H)$ at a fixed temperature for a type-I superconductor in the superconducting state. Currents near the surface of a type-I superconductor completely screen the inside of the sample, from the applied magnetic field, up to a field called the *critical field* (denoted H_C). Screening of the field means that none of the applied magnetic field gets into the sample, and the superconductor acts like a magnetic mirror (with $B = 0$ inside the superconductor). Up to H_C , the $M(H)$ curve is linear having the largest negative slope possible. This volume magnetic susceptibility is that of a perfect diamagnet ($\chi = -1/4\pi$ in cgs units), which is an enormous value compared to most other diamagnets.

An $M(H)$ curve for an ideal type-II superconductor is shown in Figure 17b. Up to an applied field known as the lower critical field H_{C1} , a type-II superconductor behaves like a type-I superconductor. However, when the applied magnetic field H exceeds H_{C1} the magnetization begins to decrease in magnitude due to the penetration of the magnetic field into the material in the form of *flux vortices*.

The magnetization will continue to decrease up to a magnetic field value called the *upper critical field* (denoted H_{c2}). At H_{c2} and higher fields the superconductivity is suppressed and the system becomes normal (non-superconducting). The curve shown in Figure 17b is the ideal type-II superconductor $M(H)$ curve and this curve is reversible even though it is non-linear above H_{c1} . It is interesting to note that this ideal superconductor would be useless for most applications, and, in fact, no supercurrent could flow above H_{c1} in such a superconductor. For it to be useful in practical applications we must modify the superconductor in ways such that the $M(H)$ curve of the superconductor becomes irreversible (hysteretic). This can be done by introducing defects into the material, usually through an appropriate choice of preparation and processing conditions. These defects serve to pin the magnetic field lines, thereby restricting their motion. It is the motion of the field lines that usually limits the current density above H_{c1} .

Introducing defects into an ideal superconductor changes the $M(H)$ curve from that of Figure 17b to one like that of Figure 18 which shows little evidence of H_{c1} ; furthermore, the $M(H)$ curve is definitely neither linear nor reversible. Now it is possible for a supercurrent to flow above H_{c1} , and the amount of supercurrent that can flow can be determined from the value of the magnetization. An important quantity in such superconductors is the critical current density (denoted J_c), and it is a remarkable result that a magnetic measurement can be used to determine how much electrical supercurrent (a transport property) can be carried by the superconductor. The relation between the magnetization M and J_c is called the *Bean Critical State Model* and is given by

$$J_c = s M / d,$$

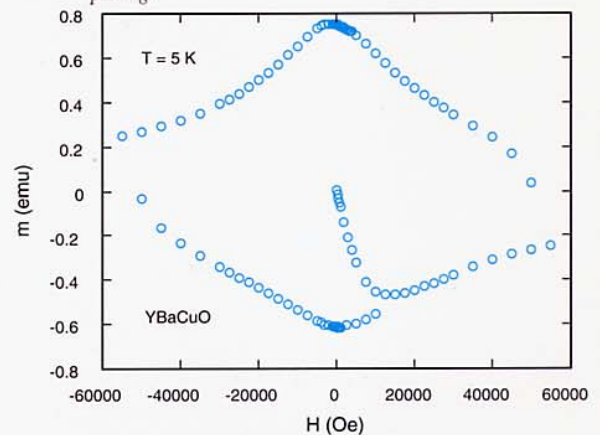
where d is the sample width or diameter and the constant s is a shape dependent constant having a value $s = 10/\pi$ for an infinite rectangular slab sample and $s = 15/\pi$ for a cylindrical sample. (This equation is for units of J_c in A/cm^2 , M in G, and d in cm.)

Another important property of a superconductor is its superconducting transition temperature (usually denoted T_c for critical temperature). This is the temperature at which the sample goes from the superconducting state to normal state upon warming. T_c usually decreases as H is increased. It is common to measure the *Meissner effect* in order to determine T_c . When an *ideal* superconductor is cooled through its superconducting transition with a very small field applied to the sample (field-cooled (FC) measurement), the magnetic field will be completely expelled from the inside of the superconductor at T_c . The expulsion of the field at T_c is the Meissner effect and it is possible to determine T_c by measuring $M(T)$ as the point at



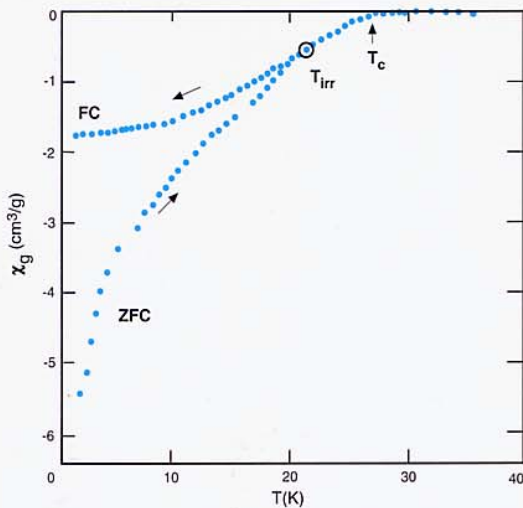
18

Magnetization as a function of field for a superconductor exhibiting irreversible magnetic behavior associated with flux pinning.



19

Magnetization as a function of temperature for the high temperature superconductor LaSrCuO . Both zero-field-cooled and field-cooled measurements are presented.



which there is a drop in M (remembering that M is negative). A plot of $M(T)$ for a high temperature superconductor is shown in Figure 19.

It is not uncommon to see a different measurement, often called *magnetic shielding* or *screening*, mistakenly called the Meissner effect. Magnetic shielding is measured by first cooling the sample to a low temperature below T_c , then turning on a magnetic field (which is also called a zero-field-cooled (ZFC) measurement). The changing magnetic field induces currents that flow as long as the sample is superconducting. The Meissner measurement and the shielding measurement both are often mistakenly used as a measure of the amount (quantity) of superconducting material in a sample. A *100% Meissner fraction*, which corresponds to a $\chi = -1/4\pi$ susceptibility value, can be used as a legitimate measure of a completely superconducting sample. However, any value of the Meissner fraction less than 100% could simply mean that there is flux pinning in the sample. The shielding measurement has other potential problems. For example, if a sample has only a thin superconducting skin and a non-superconducting center, it could conceivably produce a $\chi = -1/4\pi$ susceptibility value, since the skin could screen the whole interior of the sample to compensate the applied field H ($B = 0$ inside the sample).

UNITS

It is important to realize that the superconducting shielding results from the screening of a **volume**. The magnetization value will depend on the size of the applied field; therefore, it is the volume susceptibility χ which is important. In cgs units, perfect diamagnetism, or complete screening, has a value of $\chi = (-1/4\pi) \text{ emu}/\text{cm}^3$. Another way of viewing this is to realize that $B = 0$ in Eq. (1), requires that $-4\pi M = H$, and therefore $M/H = -1/4\pi$. In SI units, $\chi = -1$.

The critical current density (J_c) is a current per unit cross sectional area. The cgs units are A/cm^2 and the SI units are A/m^2 .

EXAMPLES AND ADVANCED TOPICS

Irreversibility Line

The region in the phase diagram between H_{c1} and H_{c2} in a type II superconductor is called either the *Abrikosov* or the *flux-vortex phase*. As discussed above, at a fixed temperature and for $H > H_{c1}$, the magnitude of M decreases as H increases. The decrease in M is due to the fact that for $H > H_{c1}$, $B \neq 0$ inside the sample, and some of the magnetic field actually penetrates into the superconductor. However, the magnetic field inside the superconductor is not distributed uniformly as it would be in most other types of material. The field that penetrates into a superconductor is *quantized* into single *quanta* of magnetic flux. A single quantum of magnetic flux

(denoted ϕ_0) has a value $\phi_0 = 2.07 \times 10^{-7}$ G-cm² in cgs units. There is a supercurrent loop associated with each magnetic flux quantum and together this comprises an entity called a *flux vortex*.

Flux vortices can be thought of as discrete lines of B. When an electrical transport current is applied to a superconductor containing flux vortices, the vortices experience a force, called the Lorentz force, which acts perpendicular to the current. If the vortices are moved by the Lorentz force, however, they generate a voltage parallel to the current that in turn produces resistive losses. To keep a supercurrent flowing requires zero resistance, therefore the flux vortices must be kept from moving. Defects in the sample can pin the vortices and thereby allow large supercurrents (large J_c values) to flow.

It was a surprise to many when it was observed that for high temperature superconductors the magnetic phase diagram between H_{c1} and H_{c2} was split into two regions and separated by a new phase boundary that is commonly referred to as the *irreversibility line* (IRL). On the upper side of the IRL below H_{c2} there is no pinning, the magnetic behavior is reversible, and no bulk supercurrents can flow. For temperatures and fields below the IRL, the magnetic behavior is irreversible and bulk supercurrents can flow. One way of measuring the IRL is to use the zero-field-cooled/field-cooled (ZFC/FC) method described in the section on ferromagnets. Below the IRL the irreversibility results in two different curves for ZFC and FC, while above the IRL there is only one value of M at a given H and T, and thus the ZFC and FC curves are superimposed as shown in Figure 19. The IRL is an important property that sets the limits on the range where a superconductor can be used in most applications. A plot showing the relationship between the IRL and the critical fields is presented in Figure 20.

Minor Loops

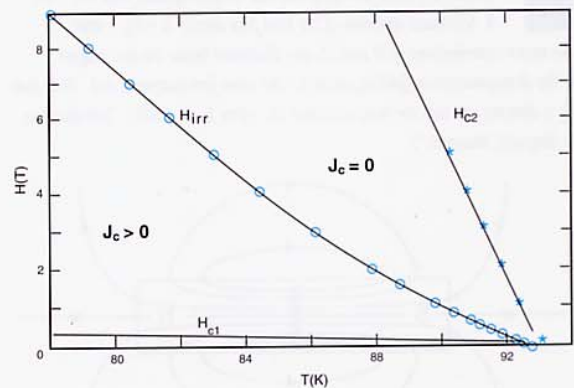
When trying to measure irreversible magnetic properties in a sample, it is important to be able to control the sample's field history. Determining J_c using a magnetic measurement requires that the critical state be established in the sample. To establish the critical state the field should be changed monotonically and then should not change at all during the measurement scan.

If the length of an MPMS measuring scan is too long, the sample will experience a significant change in the value of the magnetic field during the scan. This occurs because the field in a superconducting solenoid changes with position. Over a long scan length, the sample experiences non-monotonic field variations, and, in fact, the field at the sample oscillates as the sample moves up and down. The result is that the critical state in the sample is reduced or destroyed (the sample is effectively



20

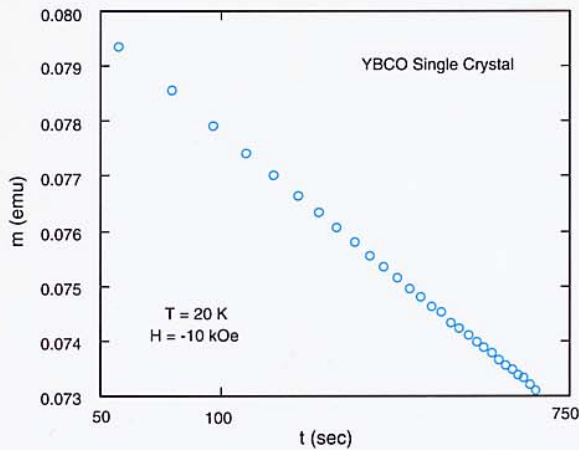
A magnetic phase diagram for the high temperature superconductor $\text{YBa}_2\text{Cu}_3\text{O}_7$. The irreversibility line separates a region (lower H and T) of finite critical current density J_c from one with $J_c = 0$.



F. DEMAGNETIZATION CORRECTIONS

21

Magnetization as a function of the logarithm of time for a thin film sample of the high temperature superconductor $\text{YBa}_2\text{Cu}_3\text{O}_7$. The slope of the curve gives a flux creep relaxation rate. The sample was cooled in zero applied field after which a field $H = -10 \text{ kOe}$ was applied and the magnetic moment measured.



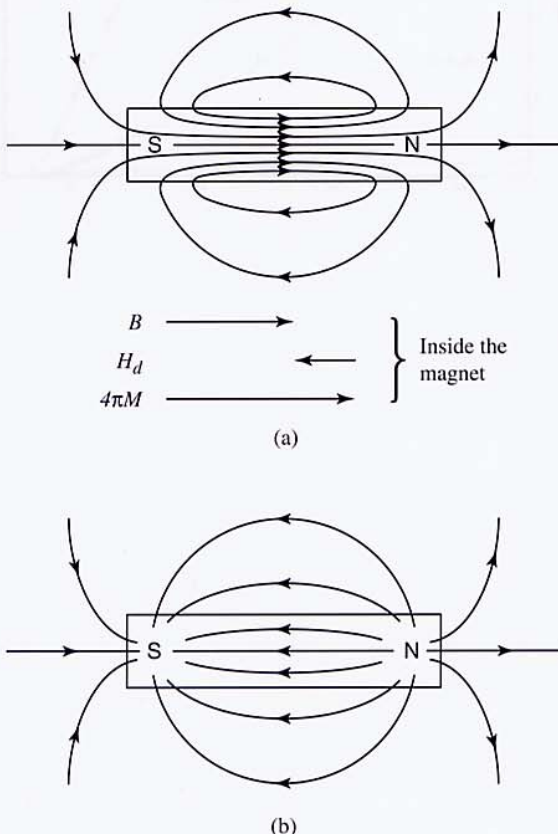
22

Shown is a hard ferromagnetic bar in zero applied field ($H_0 = 0$).

A. Schematic diagram of the total flux density $B = H_d + 4\pi M$.

The vector contributions of M and H_d are illustrated below the bar magnet.

B. The demagnetization field H_d alone for the same ferromagnetic rod. Note that H_d is directed opposite the magnetization M . [After B. D. Cullity, "Introduction to Magnetic Materials".]



demagnetized) and the magnetization value is lower than should be observed.

Thus, the J_c value is underestimated. Hence, the choice of scan length is critical when determining the magnitude of irreversible behavior. In general, the shorter the scan length the better. But from experience a scan length on the order of 2.5 cm on the MPMS seems to be a good compromise. A Technical Advisory on this subject is available.

Time Dependence

Certain types of magnetic irreversibilities have a measurable time dependence. Two of the more notable examples are high temperature superconductors and spin glasses. In superconductors the decrease in magnetization in time is attributed to flux creep. Flux creep results from the thermal activation of flux vortices out of their pinning sites. By measuring M as a function of time a flux creep rate can be determined. From a plot of M versus the logarithm of time, as shown in Figure 21, a slope related to the flux creep rate can be extracted.

F. DEMAGNETIZATION CORRECTIONS

When measuring a sample with a large magnetization value, it is often important to make *demagnetization corrections*. In this case "demagnetization" does not refer to the process of reducing the remanent magnetization, but rather is associated with the fact that the field H inside the sample depends on the shape of the sample. The origin of the demagnetization effect is usually described in terms of another magnetic field, the demagnetization field H_d , that results from the separation of hypothetical magnetic charge associated with the sample's magnetization M (see recommended reading to find a more complete discussion). The total H field inside the sample is given by $H = H_0 + H_d$, where H_0 is now the applied field produced by the current in a magnet coil and H_d is the demagnetization field. The demagnetization field is given by $H_d = -NM$ where N is the shape-dependent demagnetization factor and M is the magnetization of the material. This correction can be particularly important when measuring a strongly magnetic material. For a long, thin sample in a field parallel to its long axis, $N = 0$. For a short, flat sample in a perpendicular field, on the other hand, the demagnetization correction (NM) can be enormous. The value of N has a range $0 \leq N \leq 1$ in SI units and $0 \leq N \leq 4\pi$ in cgs units.

Shown in Figure 22 is a schematic diagram of a magnetized piece of ferromagnetic material in zero applied field ($H_0 = 0$). Figure 22a shows the B field (sum of H and M) for this ferromagnet while Figure 22b shows the field H alone. Since $H_0 = 0$, the field H inside the sample is just the demagnetization field H_d . The vectors M , B , and H_d inside the sample are also shown in Figure 22. It can be seen that for a ferromagnet H_d is negative, thereby reducing H inside the sample. In the case of a

superconductor, M is negative so H_d will be positive, leading to an increase of H inside a superconducting sample. When an external field (H_0) is applied, H_d will change with the magnetization. However, it is the total H field inside the sample ($H_0 + H_d$) that will determine M . Therefore an $M(H)$ curve should be plotted as a function of the total internal field $H = H_0 + H_d$, not the applied field H_0 .

When measuring an isotropic ferromagnetic film, for example, the $M(H_0)$ curve observed for H_0 parallel to the plane of the film will be very different than that for H_0 perpendicular to the film plane. When H_0 is perpendicular there is a large demagnetization field in the film that reduces the total H , requiring a larger applied field H_0 to saturate the film than would be required when H_0 is parallel to the film plane. However, at saturation the same value of magnetization, M_s , will be observed in both cases.

To be able to accurately apply this simple demagnetization correction to H_0 requires that the demagnetization field be uniform throughout the sample. The only sample shape for which a uniform field can exist throughout the sample is an ellipsoid. Therefore it is common practice to approximate the demagnetizing factor N for a sample by considering the "maximum-enclosed-ellipsoid," which is the ellipsoid with shape and dimensions that allow it to be enclosed in the sample and fill the maximum volume. Tables and plots of calculations of N values for ellipsoids are available (see recommended reading). Since most samples are not ellipsoids, this correction method should be considered only approximate. Sometimes materials are shaped into spheres so that this correction method can be used more accurately.

G. MAGNETIC CHARACTERIZATION OF A NEW MATERIAL

When presented with a new or unknown material, one often wants to quickly determine the general magnetic properties of the sample. The following procedure comes with no guarantees, but rather is intended as a systematic plan to help identify the magnetic behavior present in the sample. It is also only a starting point, because the more complete characterization of a sample typically requires detailed measurements once the regions of particular interest have been identified.

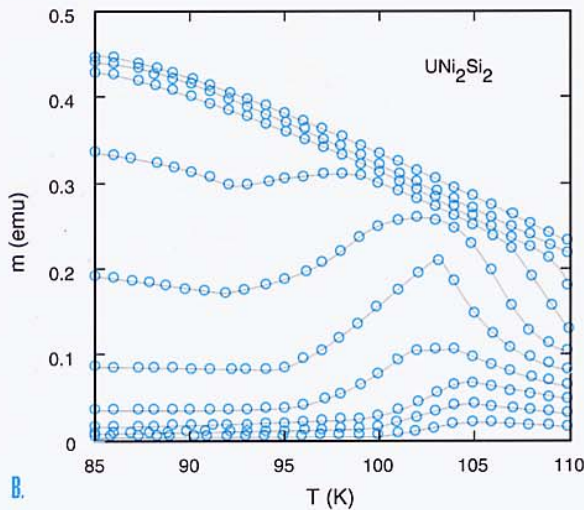
After determining the safe range of temperatures for the sample, an $M(T)$ sweep with a very low magnetic field ($H \sim 50$ to 100 Oe) should be run over the full temperature range. A temperature resolution of 5 K at low temperature and 10 K at higher temperatures is often suitable. Both superconductivity and ferromagnetism can stand out in such a scan. If one of these properties is identified, detailed measurements of that property can proceed.

G. MAGNETIC CHARACTERIZATION OF A NEW MATERIAL

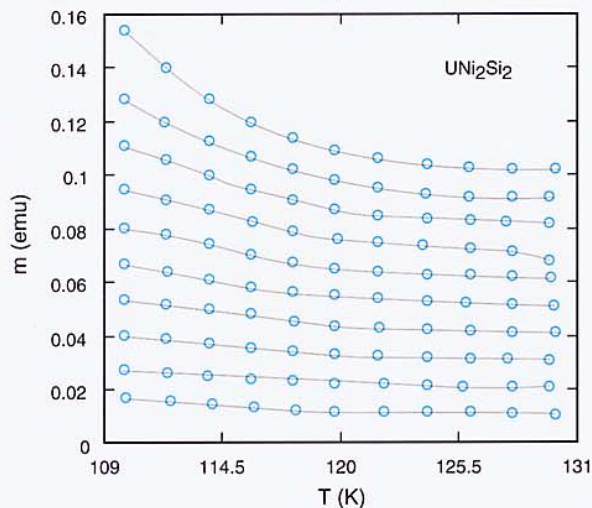
23

Magnetization as a function of temperature for UNi_2Si_2 at a series of evenly spaced applied magnetic fields. The fields range from $H = 5000$ to $H = 50000$ Oe in steps of 5000 Oe. A) The temperature range from 85 to 110 K where a metamagnetic transition region exists (from 85 to about 103 K) and a regular ferromagnetic region exists (from about 103 to about 110 K). In a metamagnetic transition the system goes from antiferromagnetic to ferromagnetic. At the lower temperatures there is a cluster of points at the lower field. The lower field cluster has an $M(H)$ curve characteristic of an antiferromagnet. Then there is a sharp increase in magnetization followed by another cluster of points at the highest fields. The cluster at the high fields is the magnetic saturation associated with a ferromagnet while in between is the transition from one magnetic behavior to the other. B) In the region near and above the ferromagnetic transition the spacing of the points at a given temperature suggest paramagnetic behavior.

A.



B.



Depending on the available time, the next procedure in a general search would be to measure $M(T)$ again over the full temperature range but now at a series of equally spaced values of H (eg. $\Delta H \sim 5$ kOe). The advantage of this kind of plot can be seen in Figure 23, for a sample of UNi_2Si_2 . If the $M(H)$ curve at a given temperature is linear, then the $M(T)$ curves taken with even field increments will be evenly spaced. If the $M(H)$ curve saturates at a certain temperature, then the points will get closer together as M saturates. Other interesting information, like a *spin flop* or *metamagnetic transitions* can often be identified from sets of $M(T)$ plots. Detailed measurements including history dependence can then proceed more efficiently with this information at hand.

A. TABLE OF CONVERSIONS

UNITS FOR MAGNETIC PROPERTIES

Quantity	Symbol	Gaussian & cgs emu ^a	Conversion factor, C ^b	SI & rationalized mks ^c
Magnetic flux density, magnetic induction	B	gauss (G) ^d	10^{-4}	tesla (T), Wb/m ²
Magnetic flux	Φ	maxwell (Mx), G·cm ²	10^{-8}	weber (Wb), volt second (V·s)
Magnetic potential difference, magnetomotive force	U, F	gilbert (Gb)	$10/4\pi$	ampere (A)
Magnetic field strength, magnetizing force	H	oersted (Oe), ^e Gb/cm	$10^3/4\pi$	A/m ^f
(Volume) magnetization ^g	M	emu/cm ^{3h}	10^3	A/m
(Volume) magnetization	$4\pi M$	G	$10^3/4\pi$	A/m
Magnetic polarization, intensity of magnetization	J, I	emu/cm ³	$4\pi \times 10^{-4}$	T, Wb/m ²ⁱ
(Mass) magnetization	σ, M	emu/g	$\frac{1}{4\pi \times 10^{-7}}$	A·m ² /kg Wb·m/kg
Magnetic moment	m	emu, erg/G	10^{-3}	A·m ² , joule per tesla (J/T)
Magnetic dipole moment	j	emu, erg/G	$4\pi \times 10^{-10}$	Wb·m ⁱ
(Volume) susceptibility	χ, κ	dimensionless, emu/cm ³	$\frac{4\pi}{(4\pi)^2} \times 10^{-7}$	dimensionless henry per meter (H/m), Wb/(A·m)
(Mass) susceptibility	χ_ρ, κ_ρ	cm ³ /g, emu/g	$\frac{4\pi \times 10^{-3}}{(4\pi)^2} \times 10^{-10}$	m ³ /kg H·m ² /kg
(Molar) susceptibility	$\chi_{\text{mol}}, \kappa_{\text{mol}}$	cm ³ /mol, emu/mol	$\frac{4\pi \times 10^{-6}}{(4\pi)^2} \times 10^{-13}$	m ³ /mol H·m ² /mol
Permeability	μ	dimensionless	$4\pi \times 10^{-7}$	H/m, Wb/(A·m)
Relative permeability ^j	μ_r	not defined		dimensionless
(Volume) energy density, energy product ^k	W	erg/cm ³	10^{-1}	J/m ³
Demagnetization factor	D, N	dimensionless	$1/4\pi$	dimensionless

a. Gaussian units and cgs emu are the same for magnetic properties. The defining relation is $B = H + 4\pi M$.

b. Multiply a number in Gaussian units by C to convert it to SI (e.g., $1 \text{ G} \times 10^{-4} \text{ T/G} = 10^{-4} \text{ T}$).

c. SI (*Système International d'Unités*) has been adopted by the National Bureau of Standards. Where two conversion factors are given, the upper one is recognized under, or consistent with, SI and is based on the definition $B = \mu_0(H + M)$, where $\mu_0 = 4\pi \times 10^{-7} \text{ H/m}$. The lower one is not recognized under SI and is based on the definition $B = \mu_0 H + J$, where the symbol I is often used in place of J .

d. $1 \text{ gauss} = 10^5 \text{ gamma } (\gamma)$.

e. Both oersted and gauss are expressed as $\text{cm}^{-1/2} \cdot \text{g}^{1/2} \cdot \text{s}^{-1}$ in terms of base units.

f. A/m was often expressed as "ampere-turn per meter" when used for magnetic field strength.

g. Magnetic moment per unit volume.

h. The designation "emu" is not a unit.

i. Recognized under SI, even though based on the definition $B = \mu_0 H + J$. See footnote c.

j. $\mu_r = \mu/\mu_0 = 1 + \chi$, all in SI. μ_r is equal to Gaussian μ .

k. $B \cdot H$ and $\mu_0 M \cdot H$ have SI units J/m³; $M \cdot H$ and $B \cdot H/4\pi$ have Gaussian units erg/cm³.

B. RECOMMENDED READING***Introduction to Magnetic Materials,***

B. D. Cullity, Addison-Wesley, 1972, ISBN# 0-201-01218-9.

This is the simplest introduction to magnetism in materials that is available. It is an engineering textbook that discusses many practical matters; an essential reference for anyone working on the magnetism of materials. Plots and tables of demagnetization coefficients are included.

The Physical Principles of Magnetism,

A. H. Morrish, R. E. Krieger, Wiley (no longer in print), 1983, ISBN# 0-88275-670-2.

This is a very complete physics textbook quantitatively describing the physical properties of magnetic materials.

Magneto-Chemistry,

R. L. Carlin, Springer-Verlag, 1986, ISBN# 0-387-15816-2.

This is an introduction to magnetism primarily in molecular systems.

Long Range Order in Solids,

R. M. White and T. H. Geballe, Academic Press, 1979, ISBN# 0-12-607777-0.

This is an advanced solid state physics textbook that discusses long range order in general and in various specific cases (i.e., magnetic and superconducting transitions). It is an excellent source of references to the literature on magnetism.

Introduction to Superconductivity,

A. C. Rose-Innes and E. H. Rhoderick, Pergamon, 1978, ISBN# 0-08-021651-8.

This is a fairly accessible development of superconductivity requiring a modest knowledge of solid state physics.

Superconductivity of Metals and Alloys,

P. G. DeGennes, Addison-Wesley, 1966, ISBN# 0-201-51007-3.

This is a graduate-level physics textbook on superconductivity and is regarded as one of the classic texts on superconductivity.

Introduction to Superconductivity,

M. Tinkham, R. E. Krieger, Pubnet, 1980, ISBN# 0-89874-049-5.

This is a graduate-level physics textbook on superconductivity and is also regarded as one of the classic texts on superconductivity.

Quantum Design, Inc.
11578 Sorrento Valley Rd
San Diego, CA 92121 USA
Tel: 1-858-481-4400 ext. 106
Fax: 1-858-481-7410
Mobile: 1-619-892-8098
Email: info@qdusa.com
Web: www.qdusa.com